AD-A093 982 DYNAMICS TECHNOLOGY INC TORRANCE CA F/G 1/3
ANALYSIS FOR OBTAINING HIGH LIFT PRESSURE DISTRIBUTIONS FOR TRA--ETC(U)
JUN 80 E JAMES, K KUSUNOSE N00014-79-C-0458
UNCLASSIFIED DT-7817-6 NL

LEVEL II

12

Dynamics Technology, Inc.

DT-7817-6

ANALYSIS FOR OBTAINING HIGH LIFT PRESSURE DISTRIBUTIONS FOR TRANSONIC AIRFOILS

FINAL REPORT

JUNE 1980

SPONSORED BY: OFFICE OF NAVAL RESEARCH
800 NORTH QUINCY STREET
ARLINGTON, VIRGINIA 22217

UNDER: CONTRACT NO. N00014-79-C-0458

BY: E. JAMES, PH.D.
K. KUSUNOSE, PH.D.

DYNAMICS TECHNOLOGY, INC.
22939 HAWTHORNE BLVD., SUITE 200
TORRANCE, CALIFORNIA 90505
(213) 373-0666

Approved for Public Release; Distribution Unlimited

This report has undergone an extensive internal review before publication, both for technical and non-technical content, by the Program Manager and an independent internal review committee.

Program Manager:

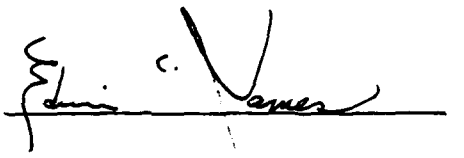

Internal Review:

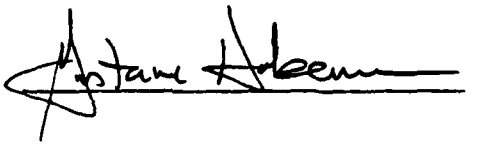

SECURITY CLASSIFICATION OF THIS PAGE (When Data Entered)

REPORT DOCUMENTATION PAGE	READ INSTRUCTIONS BEFORE COMPLETING FORM
1. REPORT NUMBER: DT-7817-6	2. GOVT ACCESSION NO.: AD-A093 982
3. RECIPIENT'S CATALOG NUMBER	
4. TITLE (and Subtitle): Analysis for Obtaining High Lift Pressure Distributions for Transonic Airfoils	5. TYPE OF REPORT & PERIOD COVERED: Technical Report
6. PERFORMING ORG. REPORT NUMBER: DT-7817-6	
7. AUTHOR(s): E. James, K. Kusunose	8. CONTRACT OR GRANT NUMBER(s): N00014-79-C-0458
9. PERFORMING ORGANIZATION NAME AND ADDRESS: Dynamics Technology, Inc. 22939 Hawthorne Blvd., Suite 200 Torrance, California 90505	10. PROGRAM ELEMENT, PROJECT, TASK AREA & WORK UNIT NUMBERS: NR 212-263
11. CONTROLLING OFFICE NAME AND ADDRESS: Office of Naval Research, Dept. of the Navy 800 North Quincy Street Arlington, Virginia 22217	12. REPORT DATE: June, 1980
	13. NUMBER OF PAGES: 91
14. MONITORING AGENCY NAME & ADDRESS(if different from Controlling Office)	15. SECURITY CLASS. (of this report): UNCLASSIFIED
	15a. DECLASSIFICATION/ DOWNGRADING SCHEDULE

16. DISTRIBUTION STATEMENT (of this Report)
Approved for public release; distribution unlimited.

17. DISTRIBUTION STATEMENT (of the abstract entered in Block 20, if different from Report)

18. SUPPLEMENTARY NOTES

19. KEY WORDS (Continue on reverse side if necessary and identify by block number)
transonic, airfoil, design, maximum lift, pressure distribution, compressible separation criterion, shocks, variational problem, turbulent boundary layer

20. ABSTRACT (Continue on reverse side if necessary and identify by block number)
This report describes the development of a method for obtaining an optimum pressure distribution over the suction side of an airfoil operating in the transonic speed regime. The pressure distribution is optimum in the sense that maximum lift on the airfoil section is desired while the flow over the airfoil remains fully attached.

The development allows for shocked and shock free flows over the airfoil with a compressible and mixed laminar-turbulent boundary layer. The boundary layer

DD FORM 1 JAN 73 1473 EDITION OF 1 NOV 65 IS OBSOLETE

SECURITY CLASSIFICATION OF THIS PAGE (When Data Entered)

is typically maintained on the verge of incipient separation over the rearward stretch of the airfoil. The pressure recovery distribution is obtained from a compressible extension of Stratford's incompressible turbulent boundary layer separation criterion which is also given in the report.

A variational problem for maximum lift is formulated and solved to yield the location of the onset of the pressure recovery and the pressure distribution forward of this point.

PREFACE

This work was supported by the U. S. Office of Naval Research under Contract No.N00014-79-C-0458. The authors would like to express their appreciation to Dr. A. M. O. Smith (Consultant) and Dr. R. Whitehead (of ONR) who helped shape our thoughts on the subject.

ABSTRACT

This report describes the development of a method for obtaining an optimum pressure distribution over the suction side of an airfoil operating in the transonic speed regime. The pressure distribution is optimum in the sense that maximum lift on the airfoil section is desired while the flow over the airfoil remains fully attached.

The development allows for shocked and shock free flows over the airfoil with a compressible and mixed laminar-turbulent boundary layer. The boundary layer is typically maintained on the verge of incipient separation over the rearward stretch of the airfoil. The pressure recovery distribution is obtained from a compressible extension of Stratford's incompressible turbulent boundary layer separation criterion which is also given in the report.

A variational problem for maximum lift is formulated and solved to yield the location of the onset of the pressure recovery and the pressure distribution forward of this point.

TABLE OF CONTENTS

LIST OF ILLUSTRATIONS

LIST OF ILLUSTRATIONS (Continued)

NOMENCLATURE

A	constant defined by (A-7)
A_0, A_1, A_2	constants defined by (16)
a	speed of sound, $\frac{\gamma p}{\rho}$
B	constant defined by (B-5)
B_1	constant defined by (A-7)
$b(n)$	constant defined by (2)
C_f	skin friction coefficient
C_L	lift coefficient
C_p^*	pressure coefficient, $1 - u_e^2/u_o^2$
$\bar{C}_p$	pressure coefficient defined by (A-47)
G	defined on page 18
$g(n)$	constant defined by (2)
$\tilde{g}(n)$	defined in (C-24)
$\hat{g}$	compressibility factor ≈0.713
H	boundary layer shape factor
K	parameter for variational procedure defined by (23)
k	parameter for variational procedure defined by (23)
$\hat{k}$	inverse power of the boundary layer velocity profile before the shock, defined by (C-12)
k_1	empirical constant obtained from turbulent boundary layer flat plate experiments, 0.684
L	lift
M	Mach number
M_e	edge Mach number based in u_e and a_e

NOMENCLATURE (Continued)

M_o	Mach number defined by $u_o/\sqrt{\gamma p_o/\rho_o}$
m	power defined in the power law expression for the comparison flow, (A-30), (=1/n)
n	inverse of the exponent of the power law assumed for the comparison flow (usually taken as 6 or 7 for shock free flows)
p	local pressure
p_e	pressure in the recovery region along the edge of the boundary layer downstream of the reference point
p_o	reference pressure
P	nondimensional pertubation pressure
R_s	Reynolds number based on u_o, ν_o and s; $u_o s/\nu_o$
R_{s_1}	Reynolds number based on u_1, n_1 and s; $u_1 s/\nu_1$
R_{s_o}	Reynolds number based on u_o, ν_o and s_o; $u_o s_o/\nu_o$
$R_{s_{so}}$	Reynolds number based on u_1,n_1 and s_{so}; $u_1 s_{so}/\nu_1$
R_{x_o}	Reynolds number based on ;u_o, ν_o, and x_o; $u_o x_o/\nu_o$
R_∞	free stream Reynolds number for unit chord length $\equiv U_\infty/\nu_\infty$
r	recovery factor (usually ≈0.9)
s	arc-length along airfoil surface based upon an equivalent flat plate length
s_c	s at $C_p^* = \frac{n-2}{n+1}$ for the shock free cases
s_o	length of flat plate necessary to duplicate the momentum thickness achieved by the airfoil where u_o occurs (equivalent flat plate length)
s_s	normal shock location on the flat plate
s_{sc}	location along an equivalent flat plate at $C_p^* = \frac{n-2}{n+1}$ for the shock case

NOMENCLATURE (Continued)

s_{so}	equivalent shock free flat plate length for the shock case
s_t	equivalent flat plate trailing edge length
T	absolute temperature
u	velocity component in free stream direction
u_c	comparison flat plate velocity profile, $u_c(s,\psi)$
u_e	streamwise flow speed along the edge of the boundary layer
u_o	streamwise flow speed at the reference point
u_t	u at the trailing edge, $u_e(1)$
$\frac{\bar{u}}{U_\infty}$	defined by (21)
v	transverse velocity component
x	arc-length measured along the top airfoil surface starting at the nose
x_o	x at the maximum velocity point on the airfoil
y	local measure of transverse distance along the surface
y_j	y at the join of inner field and far field
y_*	defined by (A-3)
$\hat{y}$	transonic y coordinate, $\hat{\delta}^{-1/3}y$
α_3, α_4	constants defined by (B-13) for the shock free cases and defined by (C-27) for the shock cases
α_5	defined by $\alpha_3 s_o$
γ	ratio of specific heats
δ	boundary layer thickness
δ_s	boundary layer thickness aft of the shock
$\hat{\delta}$	thickness to chord ratio of the airfoil

NOMENCLATURE (Continued)

ε	constant defined by (A-10)
ζ	speed ratio scaled with the reference speed u_o, u/u_o
ζ_c	defined by (A-22), $u_c(s,\psi)/u_o$
η	constant defined by (A-10)
θ	momentum thickness
θ_s	shock induced momentum thickness defined by $\int_o^{\delta(s_s^+)} \frac{\rho u}{\rho_o u_o}\left(1 - \frac{u}{u_o}\ dy\right)$
κ	von Karman constant, 0.41
Λ	pressure gradient coefficient $\left(\rho_w^{-1}\kappa^{-2}u_o^{-2}\ \frac{dp}{ds}\right)^{1/2}$
λ	coefficient defined by the power law expression for the comparison flow (A-30)
μ	defined by (B-3)
ν	kinematic viscosity, μ/ρ
ξ	constant defined by (A-10)
ρ	fluid density
ρ_e	fluid density along the edge of the boundary layer
ρ_w	fluid density along the wall
σ	defined by s/s_o
$\hat{\sigma}$	nondimensional perturbatin density
τ	shear stress
τ_w	wall shear stress
ϕ	total velocity potential

NOMENCLATURE (Continued)

ϕ	nondimensional perturbation velocity potential
ψ	stream function for compressible flow defined by (A-13)
ψ_i	limiting streamline on the inner periphery of the outer region
$( )_a$	refers to adiabatic conditions
$( )_c$	refers to conditions of comparison flat plate flow
$( )_e$	refers to conditions along the edge of the boundary layer
$( )_{tr}$	refers to conditions at the transition point
$( )_w$	refers to conditions along the wall
$( )_o$	refers to reference conditions; also refers to conditions ahead of the shock for the shock cases
$( )_1$	refers to conditions aft of the shock
$( )_\infty$	refers to freestream conditions

1. INTRODUCTION

For an aircraft to maneuver effectively in the transonic speed regime, its wing must develop high lift without incurring excessive drag. This report presents a methodology for developing high lift on airfoil sections by seeking a pressure distribution that achieves high lift while maintaining fully attached flow along the airfoil surface. Consequently, the importance of reliably predicting incipient separation over an airfoil section operating in the transonic speed regime and in identifying and understanding how the principal controlling parameters of foil shape and flow characteristics affect separation have been identified as a principal area of this investigation. This issue is particularly relevant to the primary objective of developing a rational methodology for designing a high lift wing section for transonic maneuverability. Activities have therefore concentrated upon the analysis of a turbulent boundary layer and its separation characteristics over the low pressure side of a transonic wing section. In this endeavor, a compressible separation criterion has been developed in which heat transfer effects have also been included. The criterion is similar to that of Stratford's incompressible turbulent separation criterion [1].

The procedure for determining the high lift pressure distribution follows closely that of Liebeck and Smith [2] which has led to successful high lift incompressible airfoil shapes. In fact, the variational problem for maximum lift, results in all cases (incompressible, compressible, with and without shocks) to the roof-top pressure distribution followed by a, so called, Stratford type pressure recovery. The location of the on-set of the pressure recovery and the shape of the recovery pressure distribution depend upon the free stream conditions.

Maximum lift is achieved by the shock free case for specified free stream conditions. For the same free stream conditions, a shock may

occur which will result in a reduction of lift (compared with the shock free optimum pressure distribution) and an increase in drag.

An effort is anticipated in the near future to incorporate the pressure distributions obtained herein into a transonic airfoil design code to generate high lift airfoil shapes. That effort will concentrate on obtaining practical shapes from which a high lift maneuvering wing can be designed.

Inasmuch as maximum lift also depends on the specification of a realistic pressure distribution on the lower surface of the airfoil, the follow-on effort to this work will initially concentrate on the development of such. Determination of an appropriate lower surface pressure distribution when the upper surface distribution is specified brings up the matter of finding a compatible pressure distribution for transonic airfoil design codes. That is, in determining one that, with given free stream conditions, will satisfy the closure condition at the airfoil's trailing edge.

2. COMPRESSIBLE TURBULENT BOUNDARY LAYER SEPARATION CRITERION

A compressible turbulent boundary layer separation criterion is sought using the line of reasoning of Stratford in his original formulation [1] of an incompressible turbulent boundary layer separation criterion. His criterion is sufficiently accurate and is convenient for practical applications. These traits motivated the present attempt for an extension to account for compressibility.

The extension appears possible giving rise to a criterion having Mach number dependence on the right hand side of the external pressure and longitudinal pressure gradient expression. The form is similar to Stratford's but with slight changes in certain empirical constants, and in the definition of an appropriate pressure coefficient for a compressible fluid, C_p^*. This latter quantity is defined as

$$C_p^* = \left(1 - \frac{u_e^2}{u_o^2}\right) = \frac{\gamma}{(\gamma-1)} \frac{p_o}{\frac{1}{2}\rho_o u_o^2} \left[\left(\frac{p_e}{p_o}\right)^{\frac{\gamma-1}{\gamma}} - 1\right] \tag{1}$$

where the subscript 'o' denotes a reference condition. For an airfoil surface, the reference condition corresponds to the point on the surface where the inviscid solution achieves minimum pressure (maximum streamwise flow speed).

- γ is the ratio of specific heats of the fluid.
- p_o is the reference pressure.
- u_o is the streamwise flow speed at the reference point.
- p_e denotes the pressure in the recovery region along the edge of the boundary layer downstream of the reference point. This pressure is impressed on the boundary layer and, therefore, is assumed not to vary with transverse position within the boundary layer.
- u_e is the streamwise flow speed along the edge of the boundary layer.

The turbulent compressible Stratford type separation criterion was found to be

$$\left.\begin{aligned} \left(C_p^*\right)^{\frac{1}{4}(n-2)} \left(s\,\frac{dC_p^*}{ds}\right)^{1/2} &= g(n)\left(\frac{\rho_w}{\rho_e}\right)_a^{1/2}\left(R_s\cdot 10^{-6}\right)^{1/12} \\ g(n) &\equiv \kappa\, k_1^{n/2} b(n) \\ b(n) &\equiv 21.32\left(\frac{n-2}{n+1}\right)^{\frac{n-2}{4}}\left(\frac{3}{n^2(n+1)}\right)^{1/4} \end{aligned}\right\} \quad (2)$$

s is arc-length measured along the airfoil surface based upon an equivalent flat plate length. To obtain the origin of s the following procedure is used:

(i) Locate at the edge of the boundary layer the maximum flow speed u_0.

(ii) Determine the boundary layer momentum thickness at that point.

(iii) Consider flow past a semi-infinite flat plate at zero incidence with free stream conditions corresponding to p_0, u_0, ρ_0. Determine the length of flat plate s_0 necessary to duplicate the momentum thickness achieved by the airfoil where u_0 occurs.

(iv) The origin of s is taken to be the equivalent flat plate distance s_0 upstream from the point of maximum flow speed on the airfoil.

n is the inverse of the exponent of the power law assumed for the comparison flow (usually taken as 6 or 7 for shock free flows).

κ is the von Kármán constant = 0.41.

k_1 is an empirical constant obtained from turbulent boundary layer flat plate experiments = 0.684.

ρ_w is the fluid density along the wall.

ρ_e is the fluid density along the edge of the boundary layer.

R_s is the Reynolds number, based on u_0, s and ν_0 (the kinematic viscosity of the fluid at the reference point).

The density ratio (assuming the wall is adiabatic) $[\rho_w/\rho_e]_a$ introduces a Mach number dependence into the separation criterion since

$$\left(\frac{\rho_w}{\rho_e}\right)_a^{-1} = 1 + r\,\frac{(\gamma-1)}{2}\,M_e^2 \tag{3}$$

where

- r is the recovery factor (usually ≈ 0.9), and for turbulent boundary layers it is the cube root of the Prandtl number.
- M_e is the Mach number based on u_e (Mach number based on the inviscid solution, and therefore dependent on location s).

Appendix A of the report presents a detailed analytical development leading to the separation criterion just given. Use is made there of an outer boundary layer flow corresponding to a region near the edge of the boundary layer and an inner flow region very near the surface of the airfoil. Representations of the flow in these two limiting boundary layer regions are then patched together in an intermediate region to arrive at the separation criterion.

2.1 Procedural Summary for Obtaining the Separation Criterion

In the derivation of the separation criterion, the Prandtl mixing length hypothesis is used to represent the shear stress in the inner region close to the wing surface. An expression for the shear stress is also provided by integrating the boundary layer equations outward from the surface to the point y of the inner region where the stress is to be evaluated. Equating the two expressions gives a nonlinear first order ordinary differential equation for the velocity profile in the inner region. The solution (which can be obtained in closed form) has the following asymptotic form valid close to the surface when the wall shear stress vanishes:

$$\frac{u}{u_o} = 2\,\Lambda\sqrt{y}\left(1 + \frac{\Lambda}{2}\,B_1\sqrt{y} + O(y)\right) \;; \quad \begin{matrix} y \ll 1 \\ \tau_w = 0 \end{matrix}$$

where

$$\Lambda = \left(\rho_w^{-1}\kappa^{-2}\,u_o^2\,\frac{dp}{ds}\right)^{1/2} \tag{4}$$

$$B_1 = \left(1 + \frac{(\gamma-1)}{2}\,M_e^2\right)\left(\frac{T_e}{T_w}\right) - 1$$

M_e is the Mach number at the edge of the boundary layer.

T_e is the temperature of the fluid at the edge of the boundary layer.

T_w is the temperature of the airfoil surface.

Thus, when the turbulent boundary layer is on the verge of separating, its velocity profile tends to zero as the square root of the distance from the surface. Equation (4) characterizes the turbulent boundary layer in the inner region when the flow is about to separate.

In the outer region of the turbulent boundary layer, it is assumed that the total pressure loss along a streamline is independent of the pressure rise, a result supported by experimental results (see Grabowski, *et al.* [3]). As a consequence, the pressure loss along a stream line in the actual case is very nearly the same as on a corresponding streamline in the turbulent flat plate case where the pressure is constant. The characterization of the velocity profile in the outer region is given by the Bernoulli equation applied along streamlines where the pressure is assumed related to the density isentropically.

To evaluate the constant of the Bernoulli equation, a comparison flat plate velocity profile u_c is assumed to exist (similar to the actual profile) and such that, at the location along the airfoil surface corresponding to the beginning of the pressure recovery region, $p = p_0$ and $u = u_c$. At points downstream where $p \geq p_0$, a power law expression is assumed for u_c. This completes the description of the outer region of the turbulent compressible boundary layer on the verge of separation.

The inner and outer representations of the velocity profile join at some intermediate location y_j determined by calculating the quantity $\psi(\frac{\partial \zeta}{\partial y})^3$ in each of the regions and equating. Here, ψ is the streamfunction and $\zeta \equiv u/u_0$ is the speed ratio. The relationship between u and u_c at the join is determined by a similar procedure from the expression $\zeta^2/(\psi \frac{\partial \zeta}{\partial y})$. The separation criterion (2) then follows from the Bernoulli equation.

3. COMPRESSIBLE STRATFORD FLOWS

In the previous section, a compressible separation criterion was given for turbulent boundary layers (equation (2)). From equation (2) it is possible to derive theoretical boundary-layer flows downstream of the peak velocity point where the flow is on the brink of separation or free of surface shearing stress. Such flows are obtainable, initially, by integrating the separation criterion, from $s = s_o$ where $C_p^* = 0$ to $s = s_c$ where $C_p^* = (n-2)/(n+1)$. At $s = s_c$ the inner region of the boundary layer reaches all the way to the outer edge of the boundary layer. For $s \geq s_c$, a momentum integral form is used to obtain the Stratford flow which continues the one obtained from the separation criterion.

Appendix B presents a detailed derivation of the Stratford flows and the momentum integral form used to continue the flows beyond $s = s_c$.

Treating equation (2) as an ordinary differential equation and specializing to the case when $n = 6$ (i.e., the velocity profile follows a 1/6th power law), we obtain

$$\left.\begin{aligned} C_p^*(s) &= \left[B\left(\frac{s}{s_o}\right)^{1/6} - 1\right]^{1/3} ; \qquad s \leq s_c \\ C_p^*(s) &= 1 - (\alpha_3 s + \alpha_4)^{-1/2} ; \qquad s \geq s_c \end{aligned}\right\} \tag{5}$$

where

$$B = 1.695\left(1 + r\frac{(\gamma-1)}{2}M_o^2\right)^{-1/3}\left(R_{s_o}\cdot 10^{-6}\right)^{1/18}$$

$$R_{s_o} = u_o s_o/\nu_o$$

$$s_c = \left[1 + \left(\frac{4}{7B}\right)^3\right]^6 s_o$$

$$\alpha_3 = 1.412\,\frac{B}{s_c}\left(\frac{s_c}{s_o}\right)^{1/6}\left[\left(\frac{s_c}{s_o}\right)^{1/6} - 1\right]^{-2/3}$$

$$\alpha_4 = 5.444 - \alpha_3 s_c$$

M_o is the peak Mach number which occurs at $s = s_o$.

The quantity $C_p^* = 1-(u_e/u_o)^2$ can be related to Stratford's canonical pressure coefficient (the pressure difference with respect to the minimum pressure p_o normalized with respect to the dynamic head at the minimum pressure point, $s = s_o$). That is,

$$\bar{C}_p = (p-p_o) \Big/ \frac{1}{2} \rho_o u_o^2$$

The relationship (derived from equation (A-48)) is given by

$$\bar{C}_p = \frac{2}{\gamma M_o^2} \left[\left(1 + \frac{(\gamma-1)}{2} M_o^2 C_p^* \right)^{\frac{\gamma}{(\gamma-1)}} - 1 \right] \tag{6}$$

When $M_o = 0$, it can be shown that C_p^* reduces to $\bar{C}_p$. That is,

$$C_p^* = \bar{C}_p = 1 - u_e^2/u_o^2 \quad ; \quad M_o = 0$$

The compressible Stratford flows (velocity profiles on the verge of separation) are obtained from equation (5) since

$$\frac{u_e(s)}{u_o} = \left(1 - C_p^*(s) \right)^{1/2} \tag{7}$$

Figure 1 displays $\bar{C}_p$ versus C_p^* (as given in equation (6)) for a range of peak Mach numbers M_o. It can be seen that as the Mach number increases for a given speed ratio (given C_p^*) then so also does $\bar{C}_p$. Furthermore, $\bar{C}_p$ can exceed unity in contrast to the incompressible case.

Figure 2 shows a range of compressible Stratford flows. As the peak Mach number increases, compressibility permits the attainment of larger

speed ratios (relative to the incompressible Stratford flow) at any particular point s/s_0. Consequently, for incipient separation, compressibility allows the flow to decelerate at a lesser rate than its incompressible analogue.

Figures 3 and 4 present the compressible C_p^* and adiabatic density ratio $(\rho_w/\rho_e)_a$ variations corresponding to the Stratford flows given in Figure 2. It can be seen that compressibility provides C_p^* a slower recovery than the incompressible case. Regarding the adiabatic density ratio, ρ_w decreases as the edge Mach number increases for a specified ρ_e due to viscous heating.

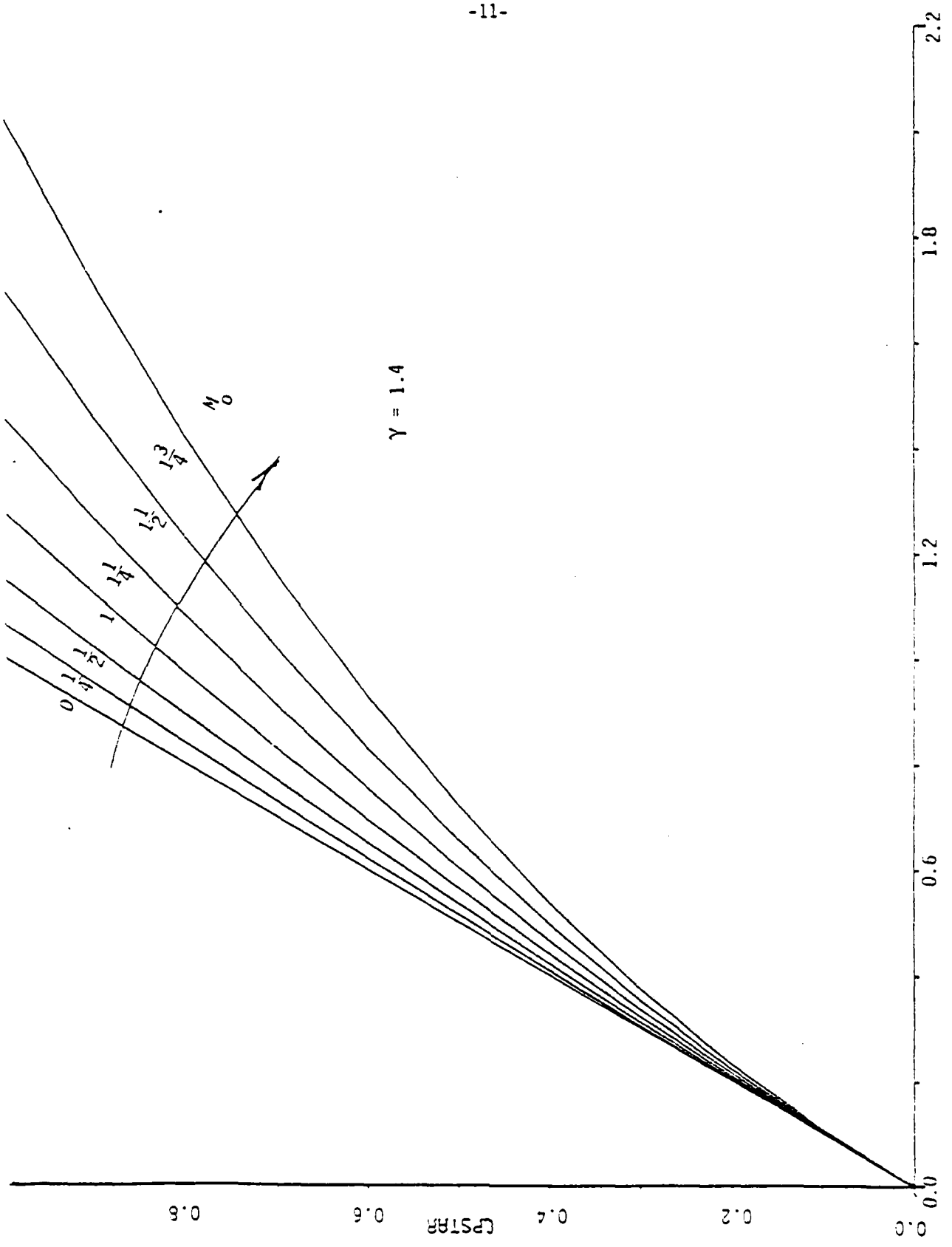

Figure 1. Variation of $\bar{C}_p$ with C_p^* for a range of peak Mach Number M_0

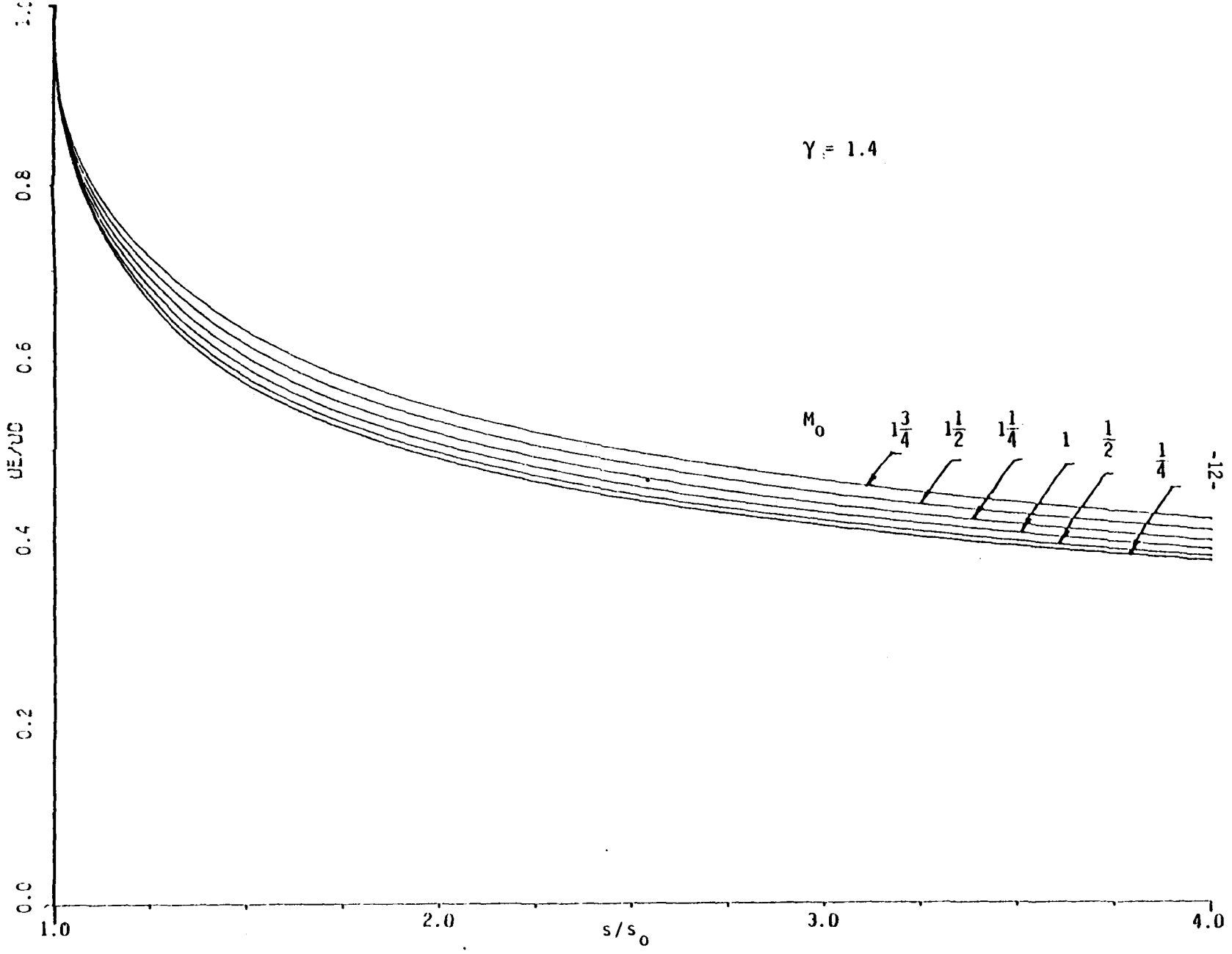

Figure 2. Compressible Stratford flows with downstream distance for a range of Mach number

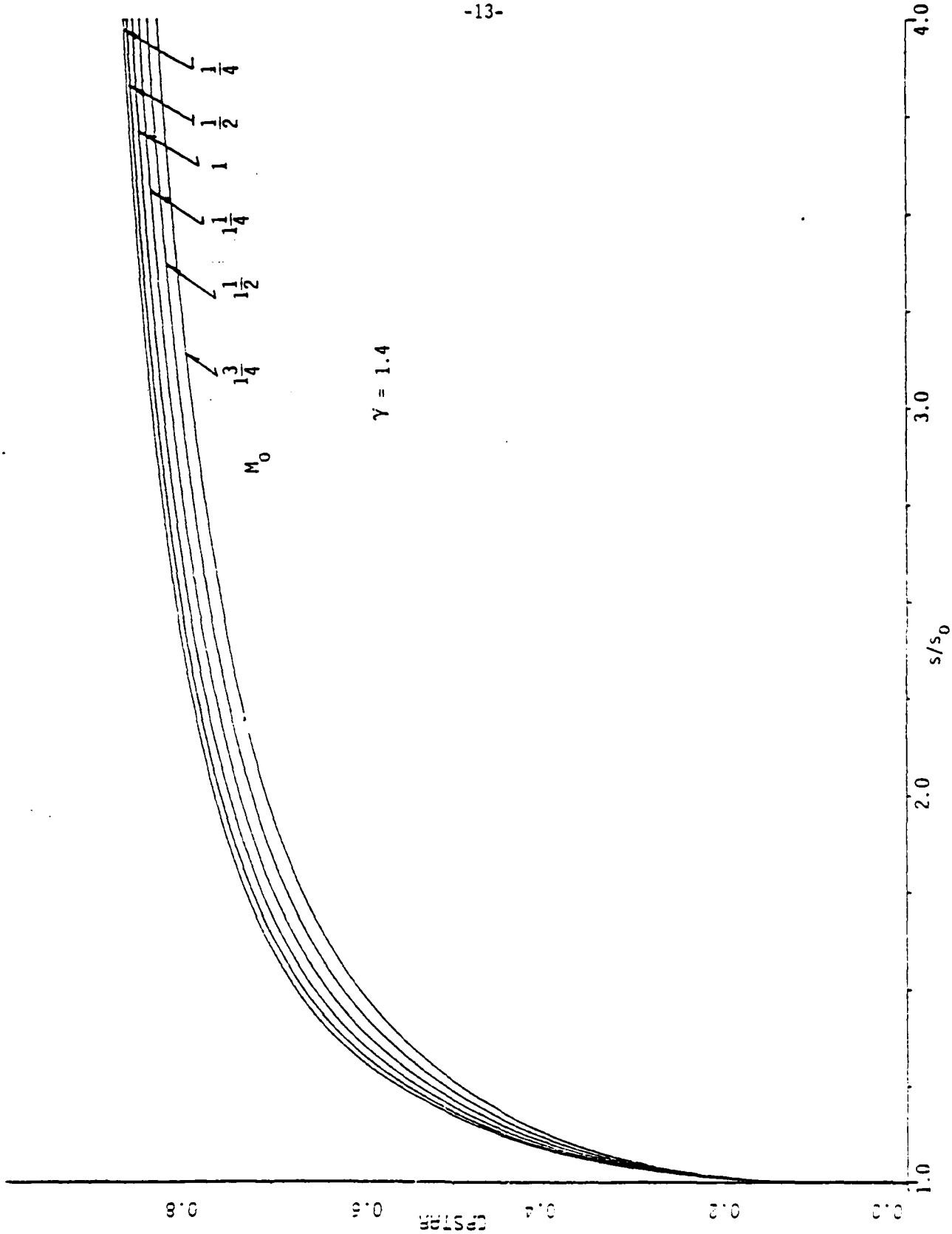

Figure 3. Stratford Type Compressible C_p^* variations with downstream distance for a range of Mach number

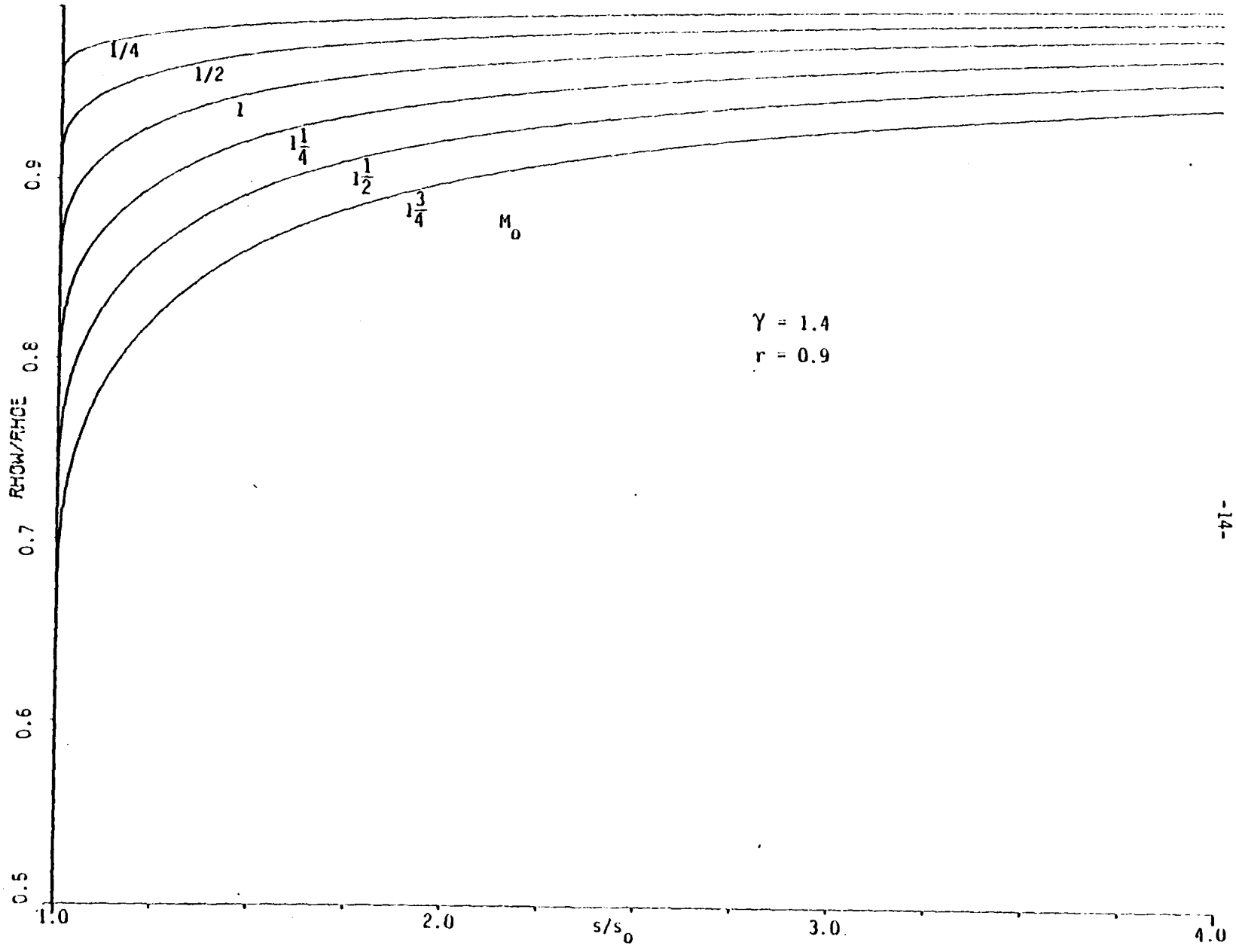

Figure 4. Stratford Type Compressible adiabatic density ratio variations with downstream distance with Mach number

4. COMPARISON OF COMPRESSIBLE SEPARATION CRITERIA

In addition to Stratford's original turbulent incompressible separation criterion, three formulae exist for the prediction of separation which purport to include the effect of compressibility. These formulae were derived or suggested by Gadd [4], Smith [5] and the criterion developed here (equation (2)).

Assessing a number of incompressible separated flows showed that a better constant on the right hand side of Stratford's incompressible criterion is 0.50 instead of 0.39. At the time Stratford developed his criterion there were limited experimental data to aid in establishing the constant. For purposes of comparing the different criteria, the 0.50 constant will be used.

The relevant formulae to be compared are:

$$\bar{C}_p \left(s \frac{d\bar{C}_p}{ds}\right)^{1/2} (10^{-6} \cdot R_s)^{-1/10} = 0.50 \qquad \text{Stratford Incompress.} \quad (8)$$

$$\left(1 - \frac{M_e^2}{M_o^2}\right)\left[s \frac{d}{ds}\left(1 - \frac{M_e^2}{M_o^2}\right)\right]^{1/2} (10^{-6} \cdot R_s)^{-1/10} = 0.50 \qquad \text{Gadd} \quad (9)$$

$$C_p^*\left(s \frac{dC_p^*}{ds}\right)^{1/2} (10^{-6} \cdot R_s)^{-1/10} = 0.50 \qquad \text{Smith} \quad (10)$$

$$C_p^*\left(s \frac{dC_p^*}{ds}\right)^{1/2} (10^{-6} \cdot R_s)^{-1/10} = 0.52 \left(\frac{\rho_w}{\rho_e}\right)_a^{1/2} (10^{-6} \cdot R_s)^{-1/60} \qquad \text{(Present)} \quad (11)$$

These formulae have been specialized to a particular exponent in a power law-type, boundary layer profile (n=6). In addition, Stratford's results have been adjusted to agree with test data as mentioned previously. All formulae have basically the same structure but equation (11) contains a density ratio and a slight Reynolds number dependence on the righ hand side.

Since Stratford's result is strictly incompressible and since compressibility affects C_p values (see Figure 4), Gadd, in view of equation (9), proposed that compressibility be accounted for by the Mach number ratio dependence of equation (9). In equation (9), M_e is the edge Mach number and M_o is the peak Mach number.

Based on studies in an AGARD paper [8], Smith suggested that velocities be used to eliminate the effect of compressibility on the pressure coefficient and equation (10) is the result. The last equation (11) is the present version which parallels Stratford's original analysis while including compressibility.

The process for predicting separation by equations (8), (9) and (10) is to observe the growth of the left hand sides - when the value reaches 0.50, then separation is assumed to occur. Equation (11) is slightly more complicated since its right hand side is not constant. However, the process for predicting separation is essentially the same. A way of comparing the formulae is to consider various decelerating flows and determine how the left hand sides behave. We begin by converting equations (8) through (11) to expressions involving only C_p^*. For Stratford's formula we define

$$C_p^* \equiv \bar{C}_p = C_p^*(M_o=0).$$

Using the energy equation, the following relation can be derived for use in Gadd's formula:

$$1 - \frac{M_e^2}{M_o^2} = \frac{\left(1 + \frac{\gamma-1}{2} M_o^2\right) C_p^*}{\left(1 + \frac{\gamma-1}{2} M_o^2 C_p^*\right)}$$

From this equation, one obtains

$$s \frac{d}{ds}\left(1 - \frac{M_e^2}{M_o^2}\right) = \frac{\left(1 + \frac{\gamma-1}{2} M_o^2\right)}{\left(1 + \frac{\gamma-1}{2} M_o^2 C_p^*\right)^2} \left(\frac{s dC_p^*}{ds}\right)$$

To simplify matters slightly, we introduce a quantity $\sigma = s/s_o$ and regard R_s and C_p^* as functions of σ. Suppose further that $R_{s_o} = 10^6$ so that

$$R_s = \frac{u_o s_o}{\nu_o} \sigma = \sigma \times 10^6$$

Consequently, equations (8) through (11) can be written

$$2A_o \left[C_p^* \left(\sigma \frac{dC_{p_o}^*}{d\sigma}\right)^{-1/2} \sigma^{-1/10}\right] = 1 \qquad \text{Stratford Incompress.} \quad (12)$$

$$2A_1 \left[C_p^* \left(\sigma \frac{dC_p^*}{d\sigma}\right)^{1/2} \sigma^{-1/10}\right] = 1 \qquad \text{Gadd} \quad (13)$$

$$2A_o \left[C_p^* \left(\sigma \frac{dC_p^*}{d\sigma}\right)^{1/2} \sigma^{-1/10}\right] = 1 \qquad \text{Smith} \quad (14)$$

$$2A_2 \left[C_p^* \left(\sigma \frac{dC_p^*}{d\sigma}\right)^{1/2} \sigma^{-1/10}\right] = 1 \qquad \text{(Present)} \quad (15)$$

where

$$A_0 \equiv 1$$

$$A_1 \equiv \left(1 + \frac{\gamma-1}{2} M_0^2\right)^{3/2} \left(1 + \frac{\gamma-1}{2} M_0^2 C_p^*\right)^{-2} \tag{16}$$

$$A_2 \equiv - \frac{\sigma^{1/60}}{1.04} \left(1 + r \frac{\gamma-1}{2} M_0^2\right)^{1/2} \left(1 + \mu C_p^*\right)^{-1/2}$$

$$\mu \equiv \frac{(\gamma-1)r}{2} \left(1 + \frac{\gamma-1}{2} M_0^2\right) \left(1 + r \frac{\gamma-1}{2} M_0^2\right)^{-1} M_0^2$$

To compare the various separation criteria, we assume a linear velocity profile in the form

$$\frac{u_e}{u_0} = (1 + \beta) - \beta\sigma \quad ; \quad \beta > 0$$

The parameter β is selected for this investigation to be 1/3 so that when $\sigma = 4$, the speed ratio vanishes. We define a quantity G as

$$G \equiv 2C_p^* \left(\sigma \frac{dC_p^*}{d\sigma}\right)^{1/2} \sigma^{-1/10} = \sqrt{8\beta}\ \sigma^{0.4} \left[1 - \left(\frac{u_e}{u_0}\right)^2\right] \left(\frac{u_e}{u_0}\right)^{1/2}$$

In Figure 5, curves of G and $1/A_i$ (i=0,1,2) versus σ are presented for a value of Mach number M_0=1.4 and β=1/3. G intersects the A_i^{-1} curves where separation is predicted.

Gadd's method predicts separation early (relative to the other two methods) for the β, M_0 constants selected. The Smith and present methods predict separation very near the same location. Consequently, the latter analysis tends to validate (and slightly refine) Smith's original contention for extending Stratford's criterion to the incompressible regime. On the basis of the analysis developed herein, the present

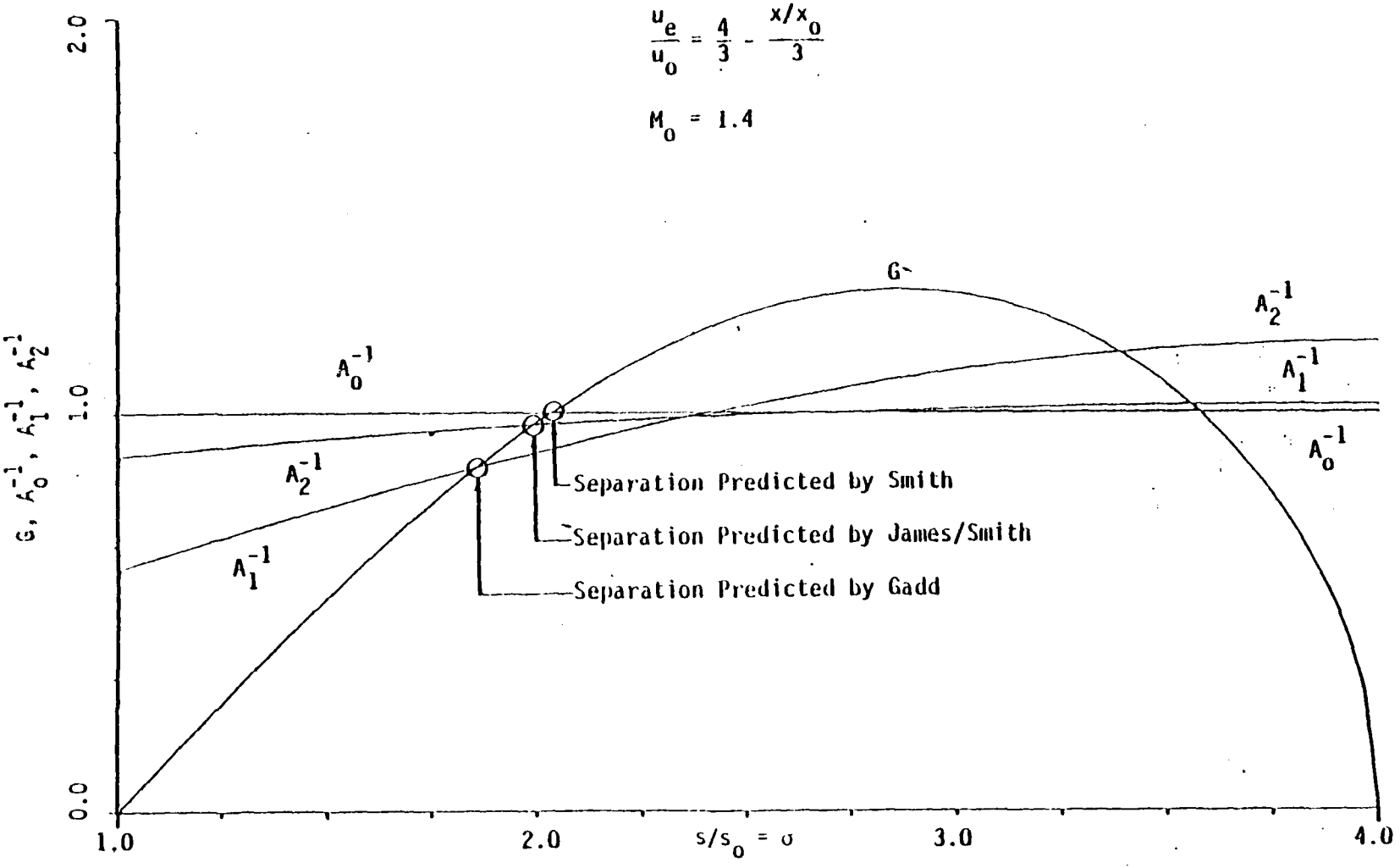

Figure 5. Example of Turbulent Separation Prediction via the Criteria of Smith (Eq. 14), Gadd (Eq. 13) and James/Smith (Eq. 15) for a Linear Speed Ratio of Slope - 1/3

formula predicts separation to occur as much as ten percent earlier than the Smith formula when the flow is such as to induce early separation (i.e., (s/s_0) near unity). When $s/s_0 > 3$, the trend reverses and Smith's formula will predict a slightly earlier separation for those flows such as to induce separation for $s/s_0 > 3$. The same basic trends prevail with respect to the Smith and Gadd formulae. However, the percent variation is seen to be considerably greater.

5. ESTIMATION OF LAMINAR RUN FOR COMPRESSIBLE BOUNDARY LAYERS

Lift generation on an airfoil section is known to be enhanced by extending the region of laminar flow on the foil. The type of flow we are striving to achieve is one that rapidly accelerates about the nose of the foil from the stagnation point x=0 to some point x on the top surface (here x is arc-length measured along the top airfoil surface starting at the front stagnation point). Thereafter it only gradually accelerates to its peak velocity which we assume is reached at $x=x_o$. (For purposes of this analysis, it is assumed that the boundary layer flow remains laminar up to the point x_{tr} where, thereafter, it spontaneously transitions to a turbulent boundary layer.) In the region of rapid acceleration near the stagnation point (zone of favorable pressure gradient) we make the assumption that the boundary layer grows incompressibly. The momentum thickness in the laminar region can then be calculated by the method of Walz [6], which follows

$$\theta^2 = \frac{0.470\nu_e}{u_e(x)} \int_0^x \left(\frac{u_e(\xi)}{u_e(x)}\right)^5 d\xi \; ; \quad x \leq x_{tr} \tag{17}$$

For the remainder of the flow up to the peak velocity we assume $u_e'(x)\approx 0$ and $u_e \approx u_o$. This is a flat plate assumption - but in this region we want to account for compressibility. Following Gruschwitz [7] (see also Reference [8], Schlichting, pages 341-344), we have for the shape factor $\hat{K}=0$ corresponding to $u_e'=0$ that

$$\frac{u_o}{2\nu_o} \frac{d}{dx}(\theta^2) = 0.2349$$

This integrates to

$$\theta^2 = \frac{0.4698\nu_o}{u_o}(x-x_*)$$

where x_* is a constant of integration.

We observe that when $u_e(x) \equiv u_0$, equation (17) reduces essentially to the previous equation when $x_* = 0$. Consequently, this result suggests that we can use equation (17) to a good approximation for the growth of a compressible boundary layer subject to a pressure gradient provided the compressible $u_e(x)$ is used. This same result has also been obtained from a more rigorous mathematical treatment but the analysis is lengthy and is not provided here.

To determine the transition point x_{tr} a simple transition criterion based on momentum thickness Reynolds number R_θ is used. Reference [9], (page 332), suggests that $R_\theta = 400$ suitably determines transition for compressible flows with pressure gradient. When this criterion is used with equation (17), the laminar run can be determined.

5.1 Equivalent Flat Plate Length

An equivalent flat plate length s_0 must be obtained for use in the separation criterion previously given. The procedure for determining an equivalent flat plate length is to find the point on a flat plate where its momentum thickness is equal to the momentum thickness at the peak velocity point on the airfoil.

In this section, we derive an expression for the turbulent momentum thickness which develops as the boundary layer flow sweeps over a specified smooth surface from a stagnation point and past the transition point where the flow is assumed to become turbulent instantaneously. In this endeavor we assume the compressible turbulent momentum thickness θ can be approximated by its incompressible analogue:

$$\theta^{\frac{n+1}{n}}\left(\frac{u(x)}{\nu}\right)^{\frac{1}{n}} = \frac{C_1}{[u(x)]^d} + C\int_{x_{tr}}^{x}\left(\frac{u(\xi)}{u(x)}\right)^d d\xi$$

where, for accelerating streams, (see Reference [8], p. 633-634) n=4, d=3.94 and C = 0.01475. In this semi-empirical result, the turbulent boundary layer begins at the point x_{tr}. To obtain the constant C_1, we use the laminar momentum thickness θ_{tr} expression derived by Walz (i.e., equation (17)). Equating the previous equation to equation (17) with x = x_{tr} and $\theta = \theta_{tr}$ gives

$$C_1 = (u_{tr})^d\left(\frac{u_{tr}}{\nu_{tr}}\right)^{\frac{1}{n}}\theta_{tr}^{\frac{n+1}{n}}$$

Therefore, the momentum thickness at the maximum velocity point x_o on the airfoil is expressed as

$$\theta_o = \left[\left(\frac{u_{tr}}{u_o}\right)^{\frac{1}{4}} + 3.94\left(\frac{\nu_o}{\nu_{tr}}\right)^{\frac{1}{4}}\theta_{tr}^{5/4} + 0.01475\left(\frac{\nu_o}{u_o}\right)^{\frac{1}{4}}\int_{x_{tr}}^{x_o}\left(\frac{u(\xi)}{u_o}\right)^{3.94} d\xi\right]^{4/5} \qquad (18)$$

The momentum thickness θ_o for a turbulent transonic boundary layer flow past a flat plate has been determined experimentally [11] to be

$$\theta_o = 0.022\left(R_{s_o}\right)^{-1/6}s_o \qquad (19)$$

To determine the equivalent flat plate length s_o of the airfoil (to the point of peak surface speed u_o), equations (18) and (19) are equated to give

$$s_o = 97.5\left(\frac{u_o}{\nu_o}\right)^{\frac{1}{5}}\left[\left(\frac{u_{tr}}{u_o}\right)^{\frac{1}{4}+3.94}\left(\frac{\nu_o}{\nu_{tr}}\right)^{\frac{1}{4}}\theta_{tr}^{\frac{5}{4}} + 0.0148\left(\frac{\nu_o}{u_o}\right)^{\frac{1}{4}}\int_{x_{tr}}^{x_o}\left(\frac{u_e(\xi)}{u_o}\right)^{3.94} d\xi\right]^{\frac{24}{25}} \quad (20)$$

For every point x (such at $0 \leq x \leq x_o$) there is an equivalent flat plate distance s (such that $0 \leq s \leq s_o$) where the correspondence is established or requiring the momentum thickness on the airfoil at x be equal to the momentum thickness on the flat plate at s. In general, s is related to x in a nonlinear fashion in the range $0 \leq x \leq x_o$. However, in the range $x_o \leq x \leq 1$, the momentum thickness growth on the airfoil is to be constrained to be the same as obtained from a compressible Stratford type flow (which invokes an equivalent flat plate analogy to the airfoil). Therefore, in that range s and x are related linearly.

6. VARIATIONAL PROBLEM FOR MAXIMUM LIFT

In this section, the variational problem for obtaining the maximum lift on a transonic airfoil section is formulated and solved. The theoretical pressure distribution has been obtained which provides the maximum lift on the airfoil assuming the flow is fully attached over the airfoil. The optimum pressure distribution obtained under the constraint of nonseparation is comprised on the upper surface of an initial flat roof-top pressure profile which prevails from the leading edge to a point x_0 where the boundary layer flow is thereafter on the brink of separation. Aft of this point, the pressure recovery is taken to be a compressible turbulent Stratford-type profile. Such a profile just avoids separation (within a certain margin of safety to allow the flow to remain attached under nominal off-design operating conditions). On the lower surface the maximum lift requirement imposes a stagnation (zero flow) surface. Consequently, the optimization problem has led to flow requirements on the upper and lower airfoil surfaces that are impossible to meet in practice. The requirements are therefore to be viewed as guide lines for achieving a high lift airfoil section. That is, certain practical modifications to the theoretically obtained pressure distribution are necessary in any realistic design, to achieve physically useful airfoil shapes. These modifications are indicated later in this report.

The solution to the variational problem formulated herein predicts the location of the point of incipient separation x_0 on the airfoil upper surface and the magnitude of the peak velocity (a constant from the leading edge to x_0).

6.1 Small Disturbance Transonic Assumption

In formulating a variational problem for obtaining the maximum lift achievable by a transonic airfoil section, use has been made of the transonic small disturbance approximation

$$\Phi(x,y) = U_\infty[x + \hat{\delta}^{2/3}\ \phi(x,\hat{y}) + O(\hat{\delta}^{4/3})]$$

$$p(x,y) = p_\infty[1 + \hat{\delta}^{2/3}\ P(x,\hat{y}) + O(\hat{\delta}^{4/3})]$$

$$\rho(x,y) = \rho_\infty[1 + \hat{\delta}^{2/3}\ \hat{\sigma}(x,\hat{y}) + O(\hat{\delta}^{4/3})]$$

where $\hat{y} = \hat{\delta}^{1/3}y$ is a compressed lateral scale, $\hat{\delta}$ is the thickness ratio and ϕ, P and $\hat{\sigma}$ are, respectively, the perturbation potential, pressure and density. See Figure 6.

The relationship between perturbation pressure and velocity is given by

$$P = -\gamma\ \phi_x$$

where $\gamma = C_p/C_v$ is the ratio of specific heats.

For a unit chord airfoil, the lift coefficient is given by

$$C_L = L/(\tfrac{1}{2}\rho_\infty U_\infty^2)$$

where $$L = \int_0^1 p_{lower}\ d\xi - \int_0^1 p_{upper}\ d\xi$$

and the subscripts "lower" and "upper" refer to the respective sides of the airfoil.

u = upper surface

ℓ = lower surface

$\hat{\delta}$ = thickness ratio

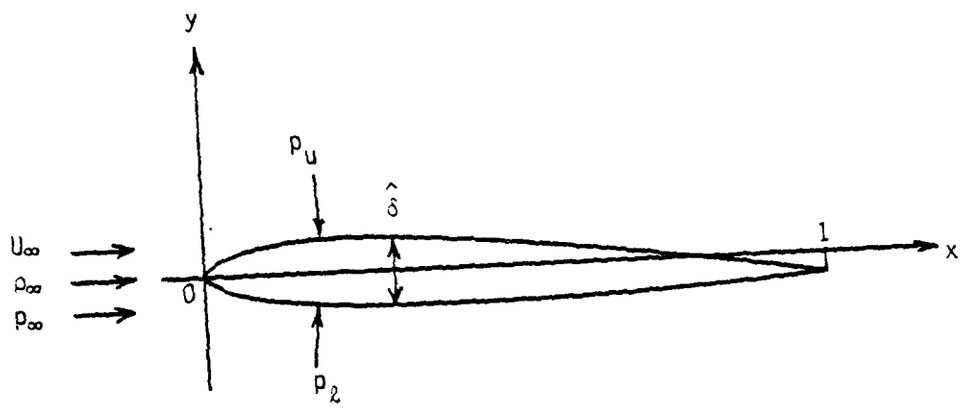

Figure 6. Uniform Flow Past a Thin Airfoil

Combining the previous four equations gives

$$M_\infty^2 C_L = \left[2\int_0^1 \left(\frac{u_e(\xi)}{U_\infty}\right) d\xi\right]_{upper} + \left[-2\int_0^1 \left(\frac{u_e(\xi)}{U_\infty}\right) d\xi\right]_{lower} + O(\hat{\delta}^{4/3})$$

where $M_\infty = U_\infty/a_\infty$ is the freestream Mach number and $a_\infty = \sqrt{\gamma\, p_\infty/\rho_\infty}$ is the corresponding speed of sound. Thus, maximizing lift is equivalent to maximizing $M_\infty^2 C_L$. To the leading order approximation, the transonic result for $M_\infty^2 C_L$ and its incompressible analogue for C_L have the identical format. Consequently, the same ideas developed by Liebeck and Smith [2] to obtain the optimum (high lift) pressure distribution can be applied to the transonic case as well. Therefore, to maximize $M_\infty^2 C_L$, we require that

$$\left| \int_0^1 \left(\frac{u_e(\xi)}{U_\infty}\right) d\xi \right|$$

on the lower surface be an absolute minimum while on the upper surface it should be a maximum. If u_e/U_∞ could be made to vanish along the entire lower surface then the optimal lower surface condition would be achieved. However, since stagnation can only occur at a point in a two-dimensional flow, a more realistic requirement is that $|u_e/U_\infty|_{lower}$ be as near zero as possible. In general, at the trailing edge $u_e = u_t > 0$ is specified.* Since flow always accelerates from a stagnation point, the lower surface problem seeks the airfoil shape that permits the flow to accelerate away from the stagnation point and achieve the trailing edge value u_t in such a way that $\int_0^1 u_e d\xi$ is as small as possible. Since the mathematical limit of zero area under the curve cannot be physically

* For a cusped trailing edge, u_t tends to U_∞. For a finite T.E. angle, the inviscid $u_t = 0$. The u_t that we specify corresponds to the tangential flow at the trailing edge external to the boundary layer. The boundary layer tends to smooth the finite T.E. angle.

met, the problem will be addressed using a "cut and try" method investigating the various practical possibilities for achieving the constraint.

The upper surface problem seeks the greatest area under the curve $\int_0^1 u_e d\xi$. This problem is controlled by boundary layer separation due to adverse pressure gradient in the recovery region.

6.2 Investigating the Quantity to be Maximized

We now focus attention on the upper surface problem and define the quantity $\overline{u}/U_\infty$ that is to be maximized.

$$\frac{\overline{u}}{U_\infty} \equiv \int_0^1 \frac{u_e}{U_\infty}\, d\xi \tag{21}$$

To obtain the largest value of $\overline{u}/U_\infty$ under the constraint that the flow remains fully attached, use is made of the limiting flow on the verge of separation. As has been developed previously, an expression for the compressible turbulent boundary layer velocity distribution that remains on the brink of separation (in terms of the equivalent flat plate length scale s) is given there by [c.f. equations (5) and (6)].

$$\frac{u_e(s)}{U_\infty} = \begin{cases} \dfrac{u_0}{U_\infty}\left[1 - \left(B\,(s/s_0)^{1/6} - 1\right)^{1/3}\right]^{1/2} & ;\ s_0 \le s \le s_c \\ \dfrac{u_0}{U_\infty}\left(\alpha_5 (s/s_0) + \alpha_4\right)^{-1/4} & ;\ s_c \le s \le s_t \end{cases} \tag{22}$$

where

$$\alpha_5 \equiv \alpha_3\, s_0$$

u_0 is the peak velocity attained at $s = s_0$, s_t denotes the equivalent flat plate trailing edge length, s_c denotes the location along an equivalent flat plate when $C_p^* = 4/7$, and B, α_4, α_5 are specified functions of the peak Mach number M_0 and equivalent flat plate Reynolds number R_{s_0}. Figure 7 illustrates the linear relationship between the airfoil arc length measured from the nose x and the equivalent flat plate length scale s along with definitions of the constants k and K (the two key parameters of the variational procedure to follow). That is,

$$\left.\begin{aligned} s - s_0 &= x - x_0 \quad ; \quad s \geq s_0 \, , \; x \geq x_0 \\ k &\equiv x_0/s_0 \\ K &\equiv s_t/s_0 \end{aligned}\right\} \tag{23}$$

The integral appearing in equation (21) can be expressed as a contribution from the accelerating region and a contribution from the pressure recovery region. Breaking up the integral in this way and using the linear relationship between s and x of equation (23) in the pressure recovery region only, gives

$$\frac{\bar{u}}{U_\infty} = \underbrace{s_0 \int_0^k \frac{u_e(\xi)}{U_\infty} \, d(\xi/s_0)}_{\text{Acceleration Region}} + \underbrace{s_0 \int_1^K \frac{u_e(s)}{U_\infty} \, d(s/s_0)}_{\text{Pressure Recovery}} \quad *$$

$$\frac{\bar{u}}{U_\infty} = \frac{\displaystyle\int_0^k \frac{u_e(\xi)}{U_\infty} \, d(\xi/s_0) + \int_1^K \frac{u_e(\xi)}{U_\infty} \, d(s/s_0)}{k + K - 1}$$

* Note we have arranged that in the acceleration region the integrand is a function of the physical arc-length [i.e., $u = u(\xi)$] and in the pressure recovery region, the integrand is a function of the equivalent flat plate length s.

u_o = maximum velocity on upper surface at $x = x_o$

s_o = equivalent turbulent flat plate length

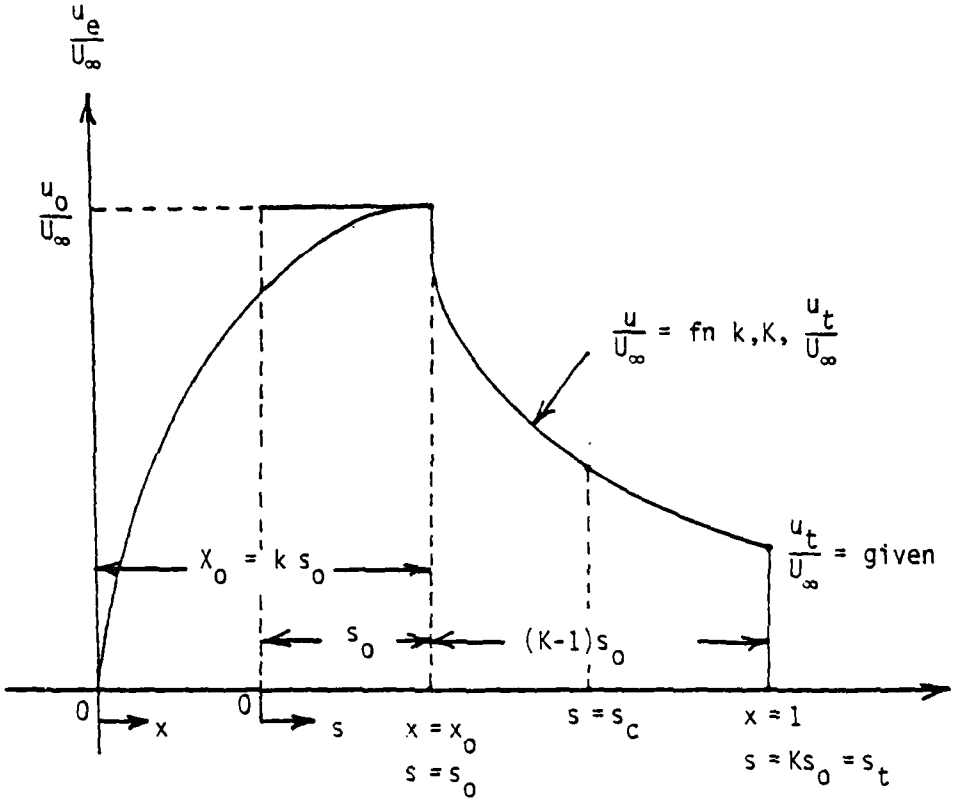

Figure 7. Upper Surface Velocity Distribution

Since the velocity distribution in the pressure recovery region is specified by equation (22), the second integral in the above expression can be written as

$$I_s(K,R_{s_o},M_o) \equiv \int_1^K \frac{u_e(s)}{U_\infty} d(s/s_o) \tag{24}$$

and therefore

$$\frac{\bar{u}}{U_\infty} = \frac{I_s(K,R_{s_o},M_o) + \int_0^k \frac{u_e(\xi)}{U_\infty} d(\xi/s_o)}{(k + K - 1)} \tag{25}$$

The Reynolds number and Mach number functional dependence enters into the I_s expression by way of equation (22). It can be shown that the peak Mach number M_o depends only on u_o for specified freestream conditions since

$$\frac{u_o^2}{2} + \frac{a_o^2}{(\gamma-1)} = \frac{U_\infty^2}{2} + \frac{a_\infty^2}{(\gamma-1)}$$

Hence,

$$M_o^2 \equiv \frac{u_o^2}{a_o^2} = \frac{u_o^2}{\left(\frac{U_\infty^2}{2} + \frac{a_\infty^2}{(\gamma-1)} - \frac{u_o^2}{2}\right)(\gamma-1)} \tag{26}$$

It can also be shown that the equivalent flat plate Reynolds number R_{s_o} depends functionally only on u_o and s_o provided the freestream conditions are known. Suppose the freestream unit length Reynolds number is $R_\infty \equiv U_\infty/\nu_\infty$. Then

$$R_{s_o} = R_\infty \frac{u_o}{U_\infty} \frac{\nu_\infty}{\nu_o} s_o \tag{27}$$

where

$$\frac{\nu_\infty}{\nu_0} = \frac{\mu_\infty}{\mu_0}\frac{\rho_0}{\rho_\infty}$$

Using the power law relationship between μ and T (see Reference [10], NACA Report 1135)

$$\frac{\mu_\infty}{\mu_0} = \left(\frac{T_\infty}{T_0}\right)^{3/4}$$

and the isentropic relationship

$$\frac{\rho_0}{\rho_\infty} = \left(\frac{T_0}{T_\infty}\right)^{1/(\gamma-1)} = \left(\frac{1 + \frac{\gamma-1}{2} M_\infty^2}{1 + \frac{\gamma-1}{2} M_0^2}\right)^{\frac{1}{(\gamma-1)}}$$

in equation (27) gives

$$R_{s_0} = R_\infty \left(\frac{1 + \frac{\gamma-1}{2} M_\infty^2}{1 + \frac{\gamma-1}{2} M_0^2}\right)^{\frac{(7-3\gamma)}{4(\gamma-1)}} \left(\frac{u_0}{U_\infty}\right) s_0 \qquad (28)$$

which displays the u_0 and s_0 dependence. Furthermore, u_0 and s_0 depend on the parameters k and K since from equation (23)

$$\left.\begin{aligned} s_0 &= 1/(K+k-1) \\ x_0 &= k/(K+k-1) \end{aligned}\right\} \qquad (29)$$

and from equation (22)

$$u_0/U_\infty = f(k,K;\ u_t/U_\infty) \qquad (30)$$

In equation (30), the trailing edge velocity ratio u_t/U_∞ is assumed given for our purposes.

As a consequence of equations (26) through (30) we have determined that the peak Mach number and the flat plate Reynolds number are functions only of k, and K provided the freestream conditions and trailing edge velocity ratio u_t/U_∞ are specified in advance. Therefore, in equation (25), $I_s(K,R_{s_0},M_0) \equiv J(k,K)$.

6.3 Two Limiting Cases of the Equivalent Flat Plate Length

The two special cases to be considered for this investigation are specified by $x_{tr}=x_0$ (full laminar run to the separation point) and $x_{tr}=0$ (full turbulent boundary layer). For the laminar run case $u_{tr}=u_0$, $\nu_{tr}=\nu_0$ and equation (20) reduces to

$$s_0 = \frac{61.98}{Re_{x_0}^{2/5}}\left[\left(\frac{U_\infty}{u_0}\right)^5 \int_0^1 \left(\frac{u_e(\xi)}{U_\infty}\right)^5 d(\xi/x_0)\right]^{3/5} x_0 \; ; \text{ laminar run} \qquad (31)$$

For a full turbulent boundary layer ($x_{tr}= 0$; $\theta_{tr}= 0$), equation (30) reduces to

$$s_0 = \frac{1.71}{Re_{x_0}^{1/25}}\left[\left(\frac{U_\infty}{u_0}\right)^{3.94} \int_0^1 \left(\frac{u_e(\xi)}{U_\infty}\right)^{3.94} d(\xi/x_0)\right]^{24/25} x_0; \text{ full turbulent} \qquad (32)$$

Since $k \equiv x_0/s_0$, equations (31) and (32) provide definitions of k for the laminar run and full turbulent cases, respectively. That is

$$\int_0^{k_\ell} \left(\frac{u_e}{U_\infty}\right)^5 d(\xi/s_o) - \left(\frac{u_o}{U_\infty}\right)^5 R_{x_o}^{2/3} \Big/ k_\ell^{2/3} \, (970.7) = 0 \tag{33}$$

$$\int_0^{k_t} \left(\frac{u_e}{U_\infty}\right)^{3.94} d(\xi/s_o) - \left(\frac{u_o}{U_\infty}\right)^{3.94} R_{x_o}^{1/24} \Big/ 1.749 \, k_t^{1/24} = 0 \tag{34}$$

where $Re_{x_o} \equiv \frac{u_o x_o}{\nu_o}$ and k_ℓ, k_t denote k for the laminar run and turbulent cases, respectively.

6.4 Variational Formulation and Solution

For both the laminar run and turbulent cases, the variational problem can be formally written by

$$\text{(maximize)} \; H[Y(n);k,K] = \frac{\int_0^k f[Y(n)]dn + J(k,K)}{G_2(k,K)} \tag{35}$$

under the constraint

$$G(k,K) + \int_0^k g[Y(n)]dn = 0 \tag{36}$$

That is, it is desired to find the function $Y(n)$ and the values of k and K which maximize the functional $H[Y(n);k,K]$ subject to a side condition, equation (36). Equations (33) and (34) are the side conditions for the two cases of interest. Compare also equations (25) and (35).

Introducing the Lagrange multiplier λ, equation (35) and (36) may be combined in the following way:

$$\tilde{H}[Y(n);k,K,\lambda] = \frac{I[Y(n),k;\lambda] + G_1(k,K,\lambda)}{G_2(k,K)} \tag{37}$$

where

$$\left.\begin{aligned} I[Y(n)k;\lambda] &= \int_0^k \left\{ f[Y(n)] + \lambda\, g[Y(n)] \right\} dn \\ G_1(k,K,\lambda) &= J(k,K) + \lambda\, G(k,K) \end{aligned}\right\} \qquad (38)$$

The first variation of $\tilde{H}$ is

$$\delta\tilde{H} = \frac{\partial\tilde{H}}{\partial I}\,\delta I + \frac{\partial\tilde{H}}{\partial G_1}\,\delta\, G_1 + \frac{\partial\tilde{H}}{\partial G_2}\,\delta\, G_2$$

Each of the variations δI, δG_1, δG_2 can be expressed in terms of the variations δY, δk and δK. Letting $\delta\tilde{H} = 0$ gives the following Euler equations

$$f_y + \lambda\, g_y = 0 \qquad ; \quad \delta Y \neq 0 \qquad (39)$$

$$\frac{\partial\tilde{H}}{\partial I}\,(f + \lambda g)\Big|_{n=k} + \frac{\partial\tilde{H}}{\partial G_1}\frac{\partial G_1}{\partial k} + \frac{\partial\tilde{H}}{\partial G_2}\frac{\partial G_2}{\partial k} = 0 \qquad ; \quad \delta k \neq 0 \qquad (40)$$

$$\frac{\partial\tilde{H}}{\partial G_1}\frac{\partial G_1}{\partial K} + \frac{\partial\tilde{H}}{\partial G_2}\frac{\partial G_2}{\partial K} = 0 \qquad ; \quad \delta K \neq 0 \qquad (41)$$

Consider first the Euler equation (39) to obtain the shape of the velocity profile in the region $0 \leq x/s_o \leq k$. From equation (25)

$$\left.\begin{aligned} Y &= u_e/U_\infty \\ f[Y] &= Y \end{aligned}\right\} \qquad (42)$$

For the laminar run case, equation (33) gives

$$g[Y] = Y^5 \tag{43}$$

Therefore, substituting (42) and (43) into (39) gives

$$1 + 5\,\lambda \left(\frac{u_e}{U_\infty}\right)^4 = 0 \qquad ; \text{ laminar case} \tag{44}$$

The δY Euler equation gives for the turbulent case (using equation (34) from which $g[Y] = Y^{3.94}$):

$$1 + 3.94\,\lambda \left(\frac{u_e}{U_\infty}\right)^{2.94} = 0 \qquad ; \text{ turbulent case} \tag{45}$$

Both equations (44) and (45) imply that u_e/U_∞ is constant in the range $0 \leq x/s_o \leq k$. But $u_e/U_\infty = u_o/U_\infty$ at $x_o/s_o = k$, so

$$u_e/U_\infty \equiv u_o/U_\infty \qquad 0 \leq x/s_o \leq k \tag{46}$$

The corresponding Lagrange multipliers can be obtained from equation (44) to (46).

Solving equations (40) and (41) provide the value of k and of K which maximize $\overline{u}/U_\infty$. Figure 8 illustrates the physical situation where the particular k and K so obtained fix the peak velocity u_o and its location x_o on the airfoil. It is difficult to obtain k,K analytically due to algebraic complexities. Consequently, a numerical procedure was used. Figure 9 and 10 display the variation of maximum theoretical lift coefficient (for both the laminar run and fully turbulent cases, respectively) with M_∞ for a range of u_t/U_∞. Figures 11 and 12 present similar results for maximum theoretical $M_\infty^2\, C_L$. It is seen that a substantial advantage exists for the laminar run case. Furthermore, the sensitivity of the results to the parameter u_t/U_∞ is quite apparent. Structural considerations at the trailing edge of an airfoil apparently limit u_t/U_∞ to about 0.9 since our perusal of airfoil data has not displayed values any greater.

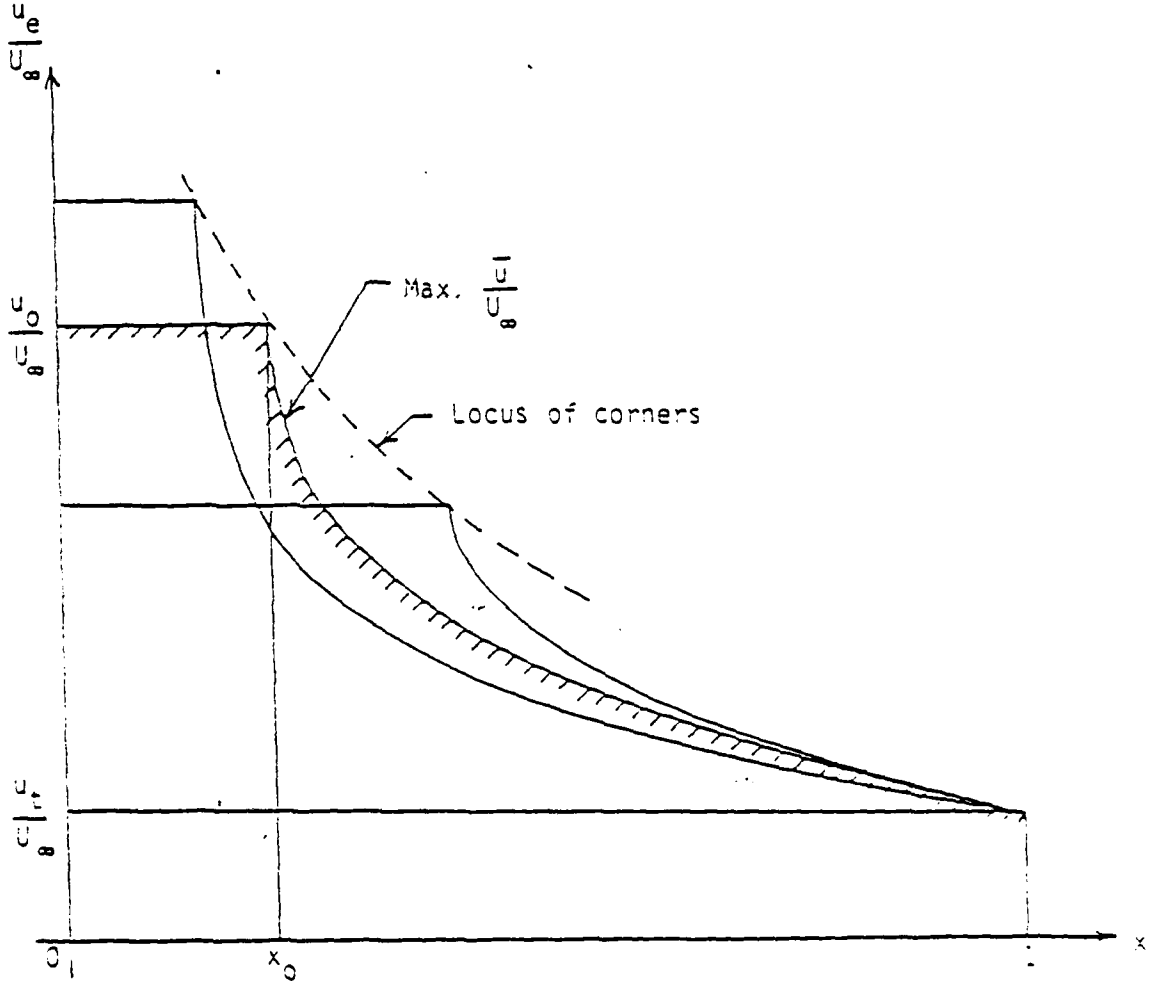

Figure 8. Family of Nonseparating Flat Rooftop Velocity Distributions for a Given u_1/U_∞ and M_∞

Laminar Run Case

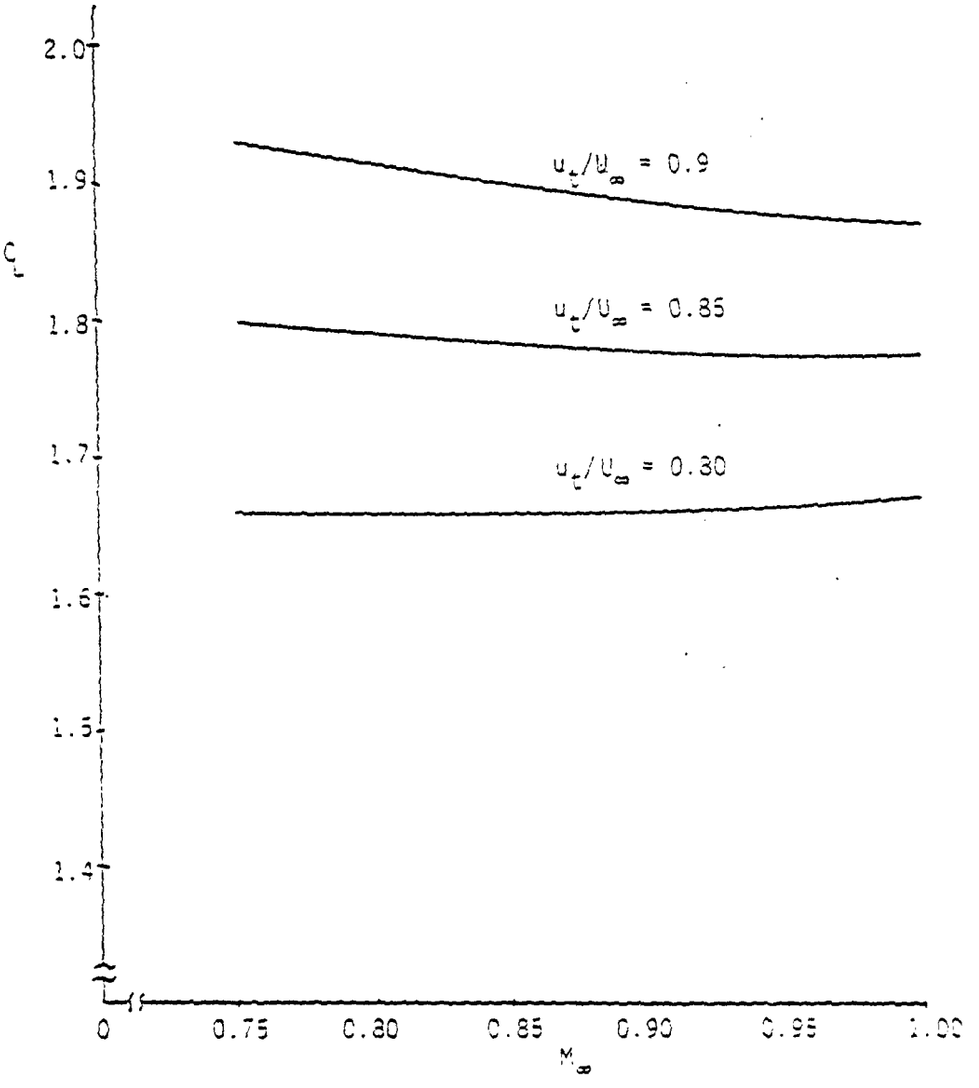

Figure 9. Variation of Maximum Theoretical Lift Coefficient Over a Range of Mach Number for Various Values of u_t/U_∞

Full Turbulent Case

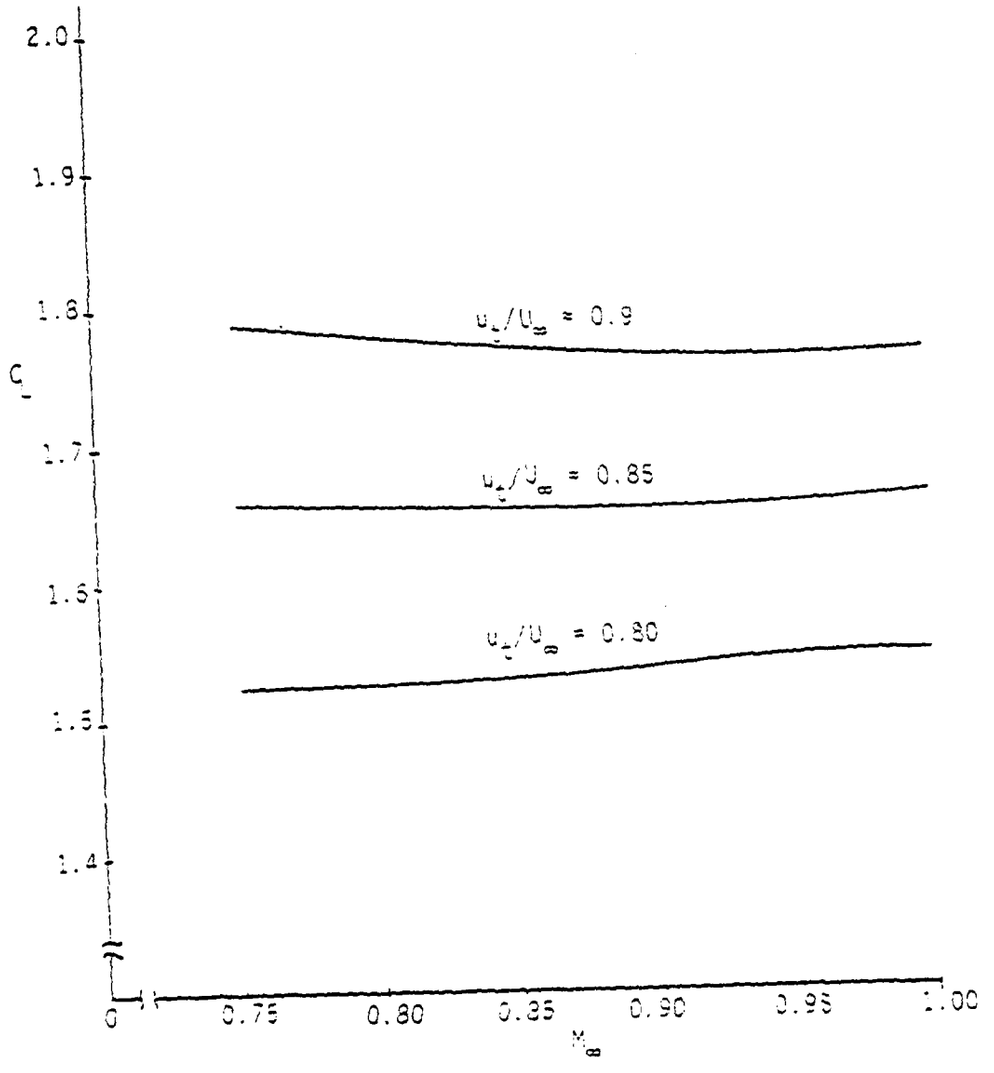

Figure 10. Variation of Maximum Theoretical Lift Coefficient Over a Range of Mach Number for Various Values of u_e/U_∞

Laminar

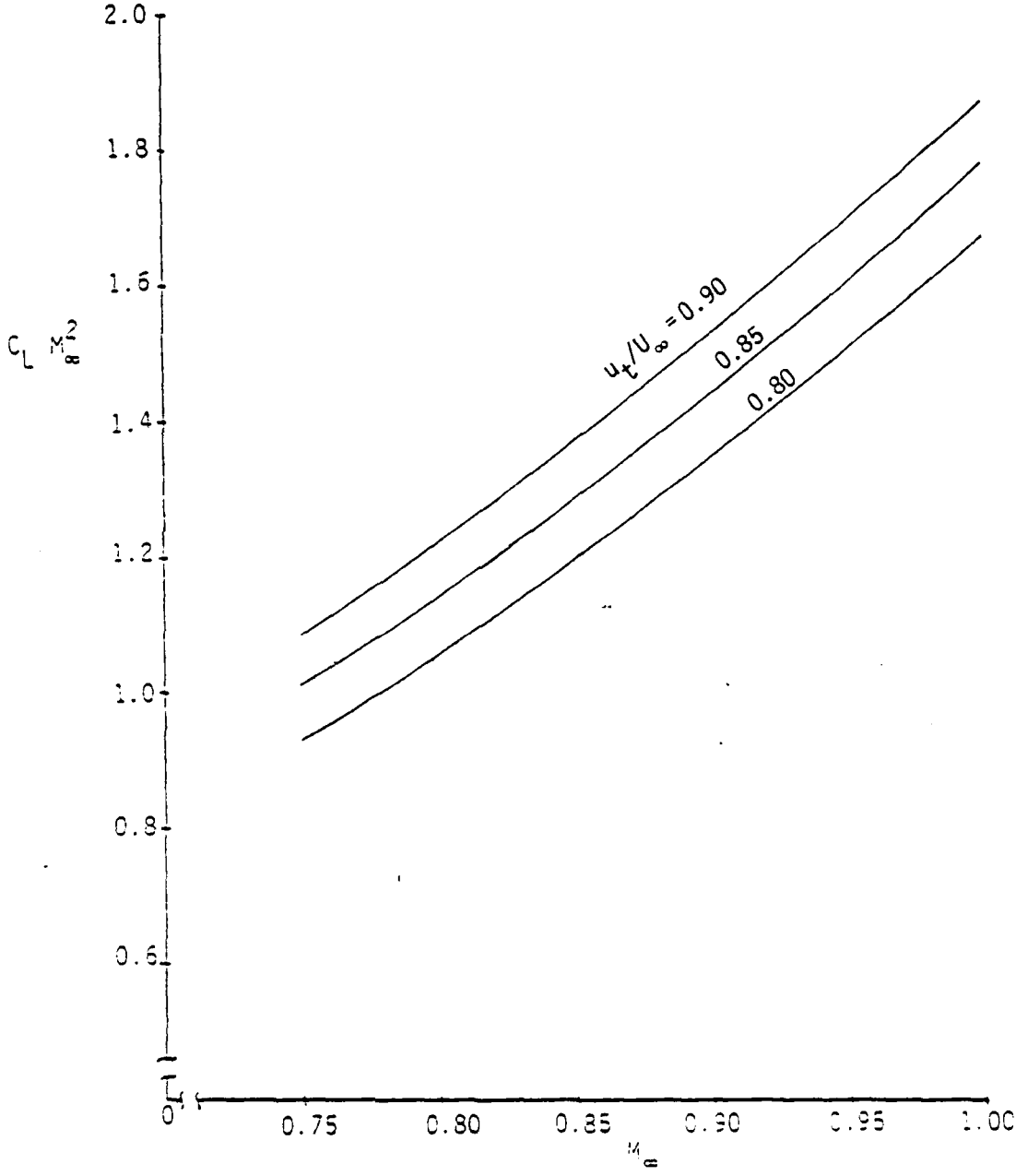

Figure 11. Variation of Maximum Theoretical $M_\infty^2 C_L$ Over a Range of Mach Number for Various Values of u_t/U_∞.

Turbulent

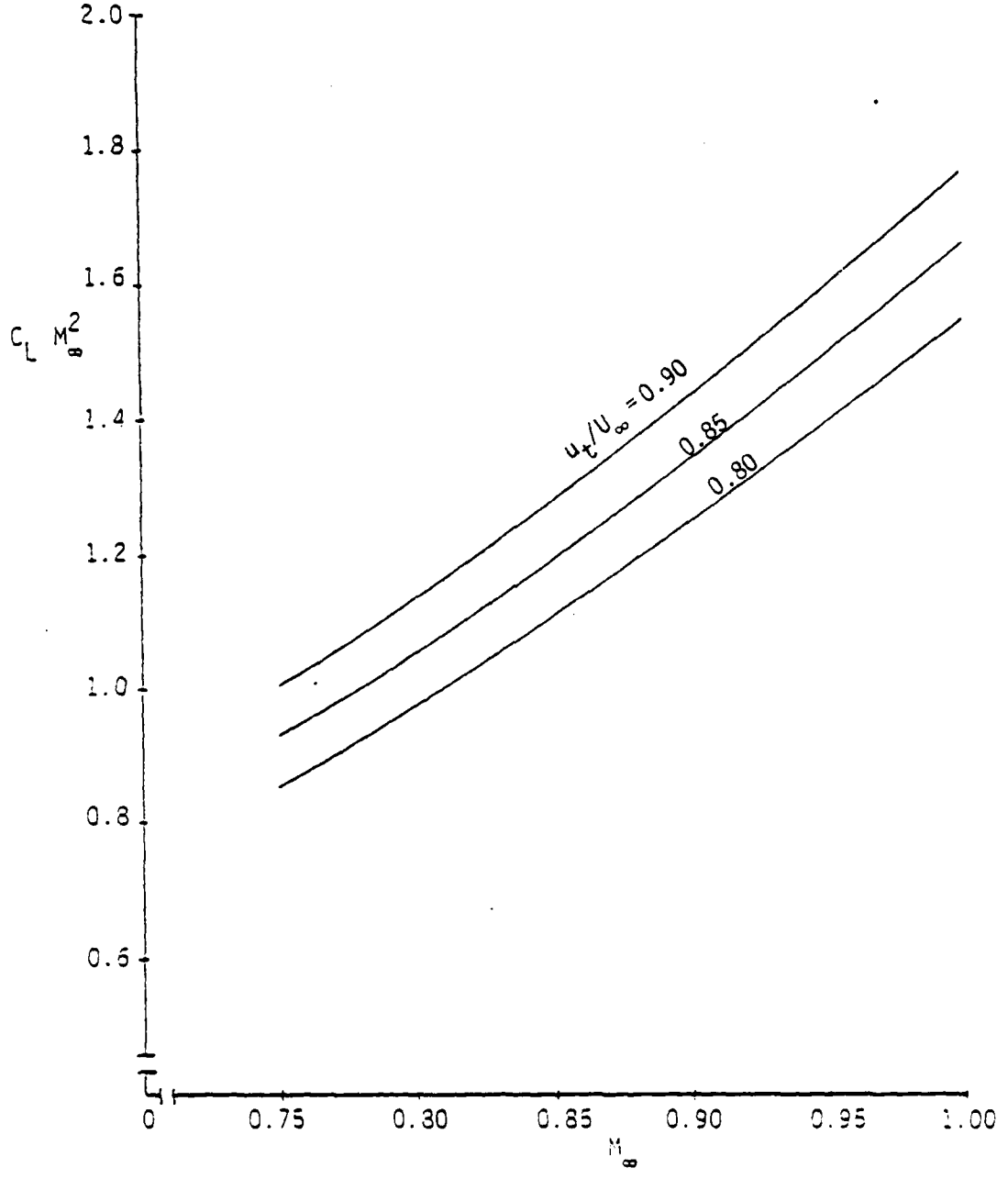

Figure 12. Variation of Maximum Theoretical $M_\infty^2 C_L$ Over a Range of Mach Number for Various Values of u_t/U_∞

6.5 Modifications To The Optimized Velocity Distribution

The analysis of the previous sections has indicated that C_L will be maximized by using a velocity distribution of the form:

$\frac{u_e}{u_\infty} = 0$ over the entire lower surface

$\frac{u_e}{u_\infty}$ given by a flat roof-top plus compressible Stratford distribution on the upper surface.

Unfortunately, this distribution will not yield a physically realizable airfoil shape due to the discontinuities present at the nose and the peak velocity point and the fact that true stagnation can not occur over the entire lower surface. Therefore, it seems necessary to modify the velocity distribution around the nose region, over the entire lower surface, and at the sudden decelerating region located in the supersonic flow on the upper surface ($x=x_o$) to avoid a possible shock there. The proposed velocity distribution modifications are indicated by the broken lines in Figure 13. Systematic variation remains yet to determine how close to the optimum pressure distribution can be obtained.

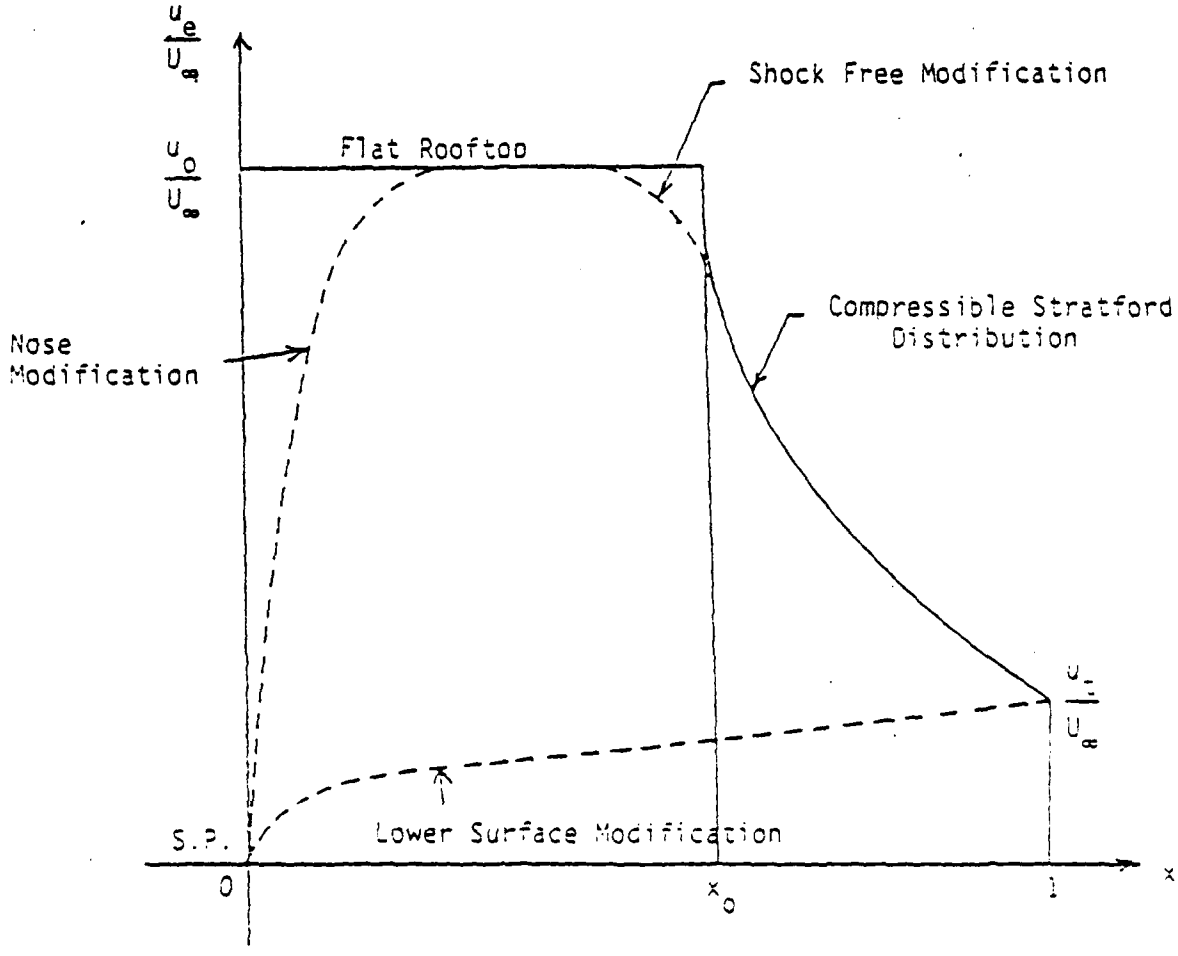

—— Optimum Velocity Distribution From the Analysis

--- Modified Velocity Distribution to Obtain a Realistic Airfoil Shape

Figure 13. Optimum and Modified Velocity Distributions

7. SHOCK CONSIDERATIONS

Our design procedure relies on relating the developing boundary layer along an airfoil surface with that on an "equivalent" flat plate (the equivalence determined via the momentum thickness). Consequently, it is important for our design procedure to have the capability of assessing the shock-boundary layer interaction through its effect on the momentum thickness. Appendix C presents a derivation of the appropriate expressions necessary to assess the shock-boundary layer interaction for incorporating the shock effect into our design procedure.

The momentum thickness after the shock θ_s was found to be related to the momentum thickness before the shock by

$$\theta_s = F(M_o;\hat{k})\ \theta_o \tag{47}$$

where

$$F(M_o;\hat{k}) \equiv 1 + \left[\frac{0.4(\hat{k}+1)(\hat{k}+2)}{(\gamma-1)\ \hat{k}\ \hat{g}}\right](1+4M_o)(1-M_o^{-2})$$

$\hat{g} \approx 0.713$ is a compressibility factor for $0.8 < M < 1.4$

$\hat{k}$ is the inverse of the power of the velocity profile before the shock. That is,

$$\frac{u}{u_o} = \left(\frac{y}{\delta_o}\right)^{1/\hat{k}}$$

If the velocity profile after the shock is described by

$$\frac{u}{u_1} = \left(\frac{y}{\delta_s}\right)^{1/n},$$

then n and $\hat{k}$ are related by

$$n = (\hat{k}+3)\left(\frac{M_1}{M_o}\right)^2 - 3 \tag{48}$$

where M_1 is the Mach number just downstream of the shock. M_1 is related to M_0 by the normal shock jump relations.

For typical values of $\hat{k}$ (≈6) and M_0 (≈1.2), the change in the momentum thickness across the shock (relative to the momentum thickness before the shock) is O(1). Equation (18) provides an expression for θ_0 for the full laminar run case and the full turbulent case.

To obtain the equivalent shock free flat plate length s_{so} (comparable to s_o in the case of no shocks), the following expression is used:

$$s_{so} = \left[\frac{\theta_s}{(0.022)}\right]^{6/5} \left(\frac{u_1}{\nu_1}\right)^{1/5} \tag{49}$$

The above equation provides an implicit relationship between the equivalent flat plate length and the shock location x_o on the airfoil.

Now, if C_p^* is defined by

$$C_p^*(s) = 1 - \left(\frac{u_e(s)}{u_1}\right)^2 \tag{50}$$

for the airfoil having a shock at x_o and a velocity u_1 immediately downstream of the shock, then the separation criterion is given precisely by equation (2) but with n determined by equation (48) and s_o replaced by s_{so}.

In this case, C_p^* for incipient separation is given by

$$\begin{aligned} C_p^*(s) &= B\left[\left(\frac{s}{s_{so}}\right)^{1/16} - 1\right]^{2n}; \qquad s \leq S_{sc} \\ C_p^*(s) &= 1 - (\alpha_3 s + \alpha_4)^{-1/2}; \qquad s \geq S_{sc} \end{aligned} \tag{51}$$

where

$$B \equiv \left\{ \frac{3gn^2(n)\left(R_{s_{so}} \cdot 10^{-6}\right)^{1/6}}{1 + \sigma \frac{(\gamma-1)}{2} M_1^2} \right\}^{2/n}$$

$$\alpha_3 = \frac{2}{3}\left(\frac{n+1}{3}\right)^3 \frac{B}{n\, s_{sc}} \left[\left(\frac{s_{sc}}{s_{so}}\right)^{1/6} - 1\right]^{\frac{2-n}{n}} \left(\frac{s_{sc}}{s_{so}}\right)^{1/6}$$

$$\alpha_4 = \left(\frac{n+1}{3}\right)^2 - \alpha_3\, s_{sc}$$

$$s_{sc} = s_{so}\left[1 + \left\{\frac{(n-2)}{B(n+1)}\right\}^{n/2}\right]^6$$

From this last equation $2 \leq n \leq \hat{k}$.

7.1 Variational Problem Including the Shock

The variational problem including a normal shock follows along the same lines as in the shockless case of Section 6. The parameters k and K (see Figure 14) are defined for the shock case by

$$k = x_o/s_{so}$$

$$K = \frac{1-x_o}{s_{so}} + 1$$

and the integral I_s (see equation (24)) is given by

$$I_s\left(K_1 \frac{u_t}{U_\infty}, R_{s_o}, M_1\right) \equiv \int_{1^+}^{K} \frac{u_e}{U_\infty}\, d\left(\frac{s}{s_{so}}\right)$$

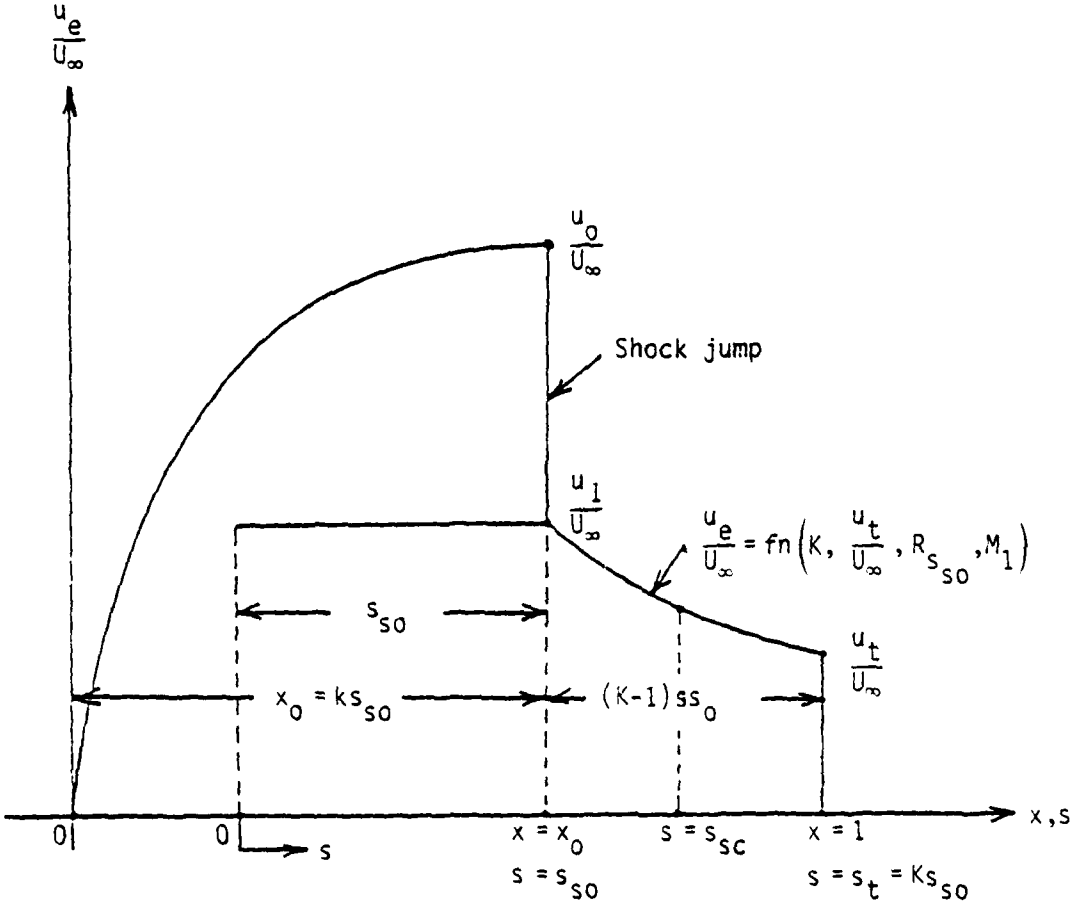

Figure 14. Upper Surface Velocity Distribution With a Shock

$$\text{where} \quad \frac{u_t}{U_\infty} = \begin{cases} \frac{u_1}{U_\infty}\left[1 - B(K^{1/6}-1)^{2/n}\right]^{1/2}; & \text{if } \frac{s_c}{s_{so}} \geq K \\ \frac{u_1}{U_\infty}\left[\alpha_5 K + \alpha_4\right]^{-1/4}; & \text{if } \frac{s_c}{s_{so}} \leq K \end{cases}$$

The location of the shock s_{so} is obtained directly from the expression $\theta_s = F(M_o;\hat{k})\theta_o$ given by equations (47) and (C-15). Using the definition of $k \equiv x_o/s_{so}$ and the above mentioned equations leads to:

$$\int_0^k \left(\frac{u_e}{u_o}\right)^{3.94} d\left(\xi/s_{so}\right) = 0.5725\ k^{-1/24}\ F(M_o;\hat{k})^{-5/4}\left(\frac{\nu_1}{u_1 x_o}\right)^{5/24}\left(\frac{\nu_o}{u_o x_o}\right)^{-1/4} \qquad (52)$$

By using the conditions along a streamline (i.e., enthalpy remains invariant, jump conditions across the shock and isentropic flow elsewhere) it can be shown that the right hand side of equation (52) depends functionally upon k, K and parametrically upon M_∞, ν_∞ and the speed ratic at the trailing edge u_t/U_∞. Furthermore, the variational formulation for the shocked flow case can be shown to reduce to exactly the form of the shockless flow case considered previously with the result that

$$u_e = u_o \quad ; \quad (0 \leq x \leq x_o \equiv k\ s_{so}) \qquad (53)$$

Consequently, the integral expression on the left hand side of equation (52) is equal to k. Therefore, equation (52) provides an implicit relationship between k and K. That is, equation (52) is of the form k=k(K) and x_o, s_{so}, u_o and $\int_o^1 u_e(x)/U_\infty\, dx_{upper}$ depend functionally only on K and parametrically on M_∞, ν_∞ and u_t/U_∞. To determine the maximum lift a numerical procedure was developed.

Numerical Results for the Maximum Lift Problem

In the shocked flow problem the order of n (the exponent of the power law of the velocity profile) is determined from

$$n = \begin{cases} (\hat{k}+3)\left(\frac{M_1}{M_0}\right)^2 - 3 \; ; & M_1 \leq 1 \\ \hat{k} \; ; & M_1 \geq 1 \quad \text{(shock free)} \end{cases}$$

It was determined that the shock solutions matched the shock free solutions only when $u_0 = a_0$ ($M_0 = 1; K = K_{sonic}$). See Figure 15. In order to calculate the shock solutions, an iteration method was employed using the exact shock free sonic solution as an initial guess. Some results are provided in Figures 16 - 18 for the trailing edge speed ratio $u_t/U_\infty = 0.9$ and for a range of free stream Mach numbers $M_\infty = 0.8$, 0.9 and 1.0. As M_∞ increases, the length of the roof-top pressure distribution is seen to increase. Furthermore, the Stratford type velocity profile exhibits less streamwise variation as the strength of the shock increases. This is expected on physical grounds since the effect of an increase in shock strength is to bring the boundary layer velocity profile closer to the condition of separation. Figure 19 shows for the trailing edge speed ratio $u_t/U_\infty = 0.9$ how the maximum lift coefficient was found to vary with free stream Mach number in the transonic speed regime for a fully turbulent boundary layer for the cases of shocked and shock free flow. The minimum percentage difference between the case with shocks and without shocks was found to be approximately 11%; with the occurrence of shocks diminishing the maximum lift coefficient.

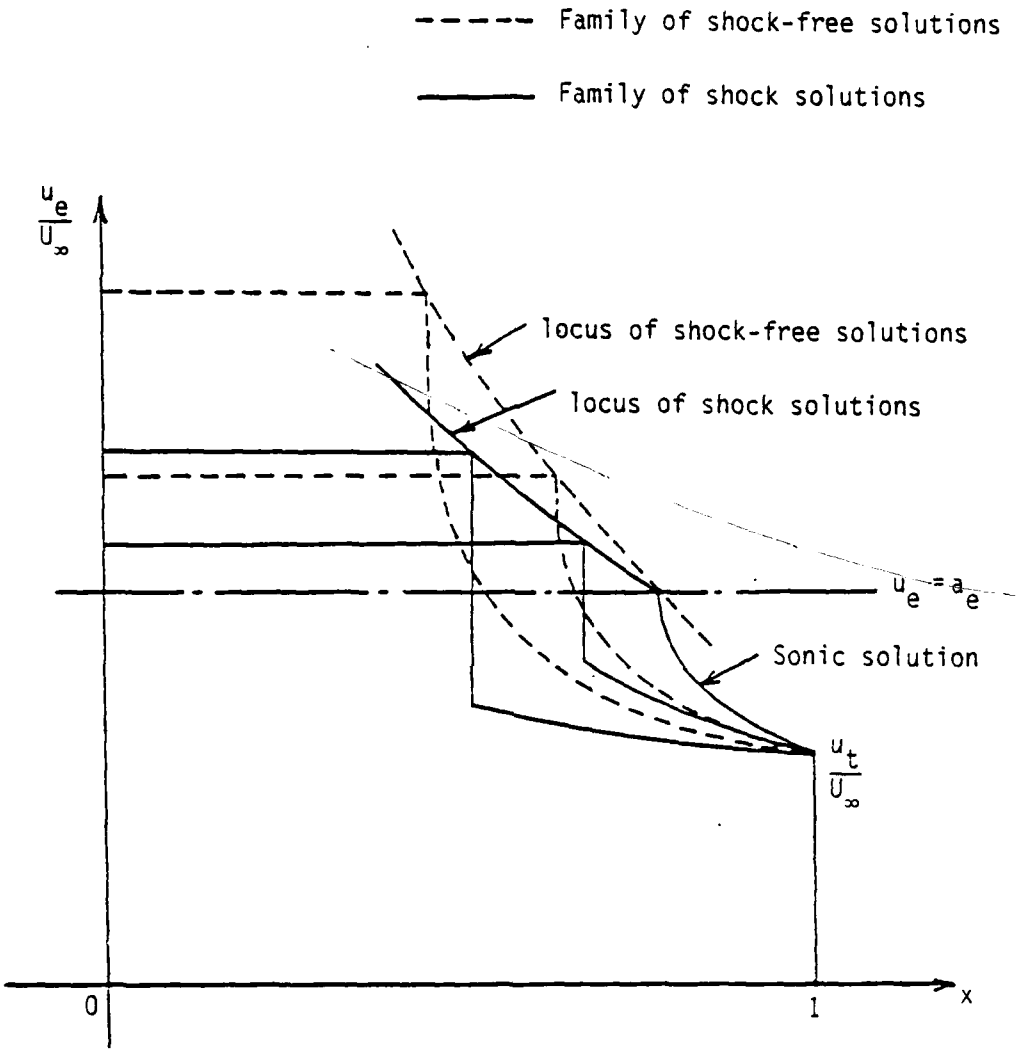

Figure 15. Velocity Distribution for Shock-Free and Shock Solutions

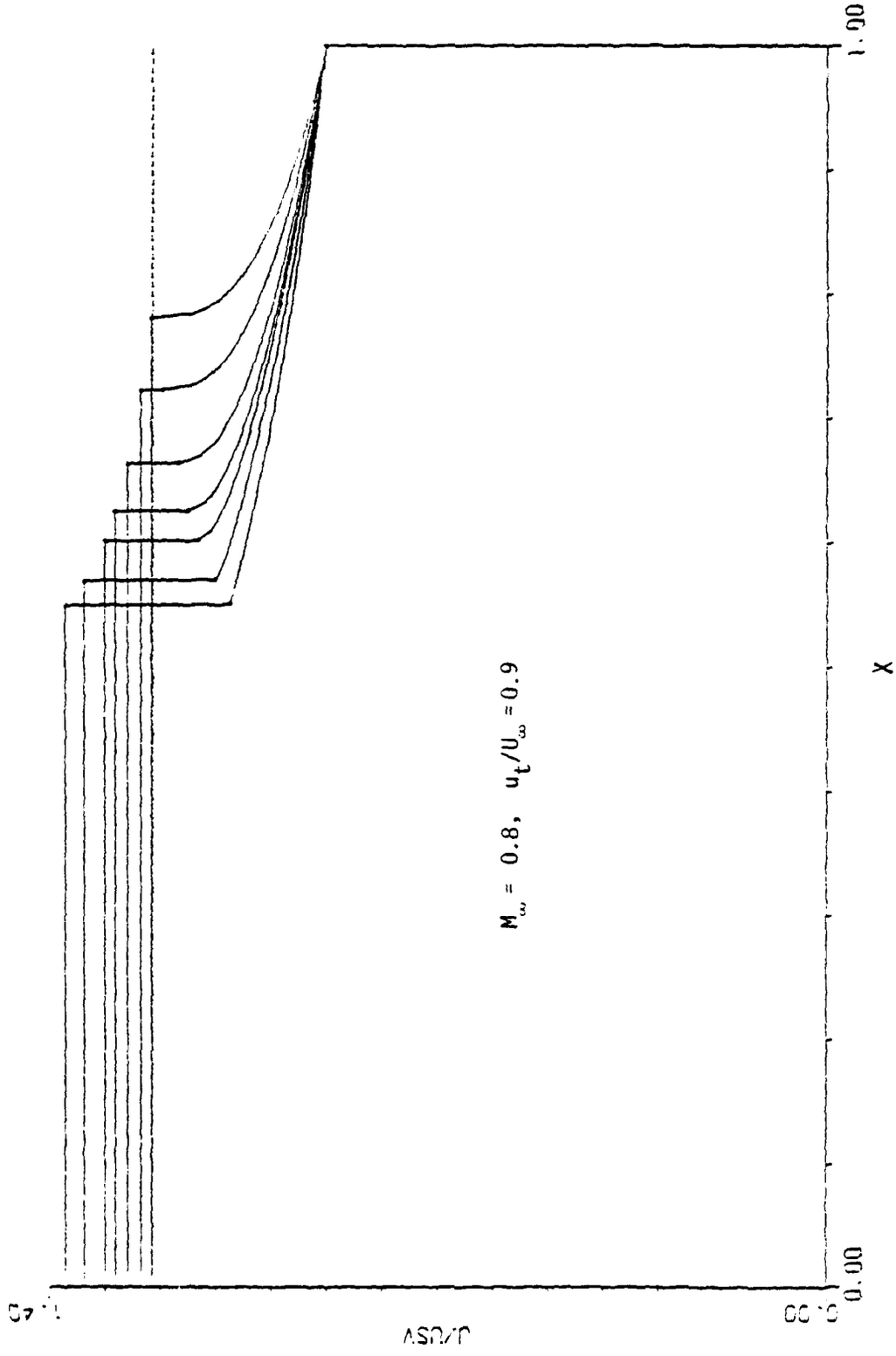

Figure 16. A Family of Shock Solutions for Given Values of M_∞ and u_t/U_∞

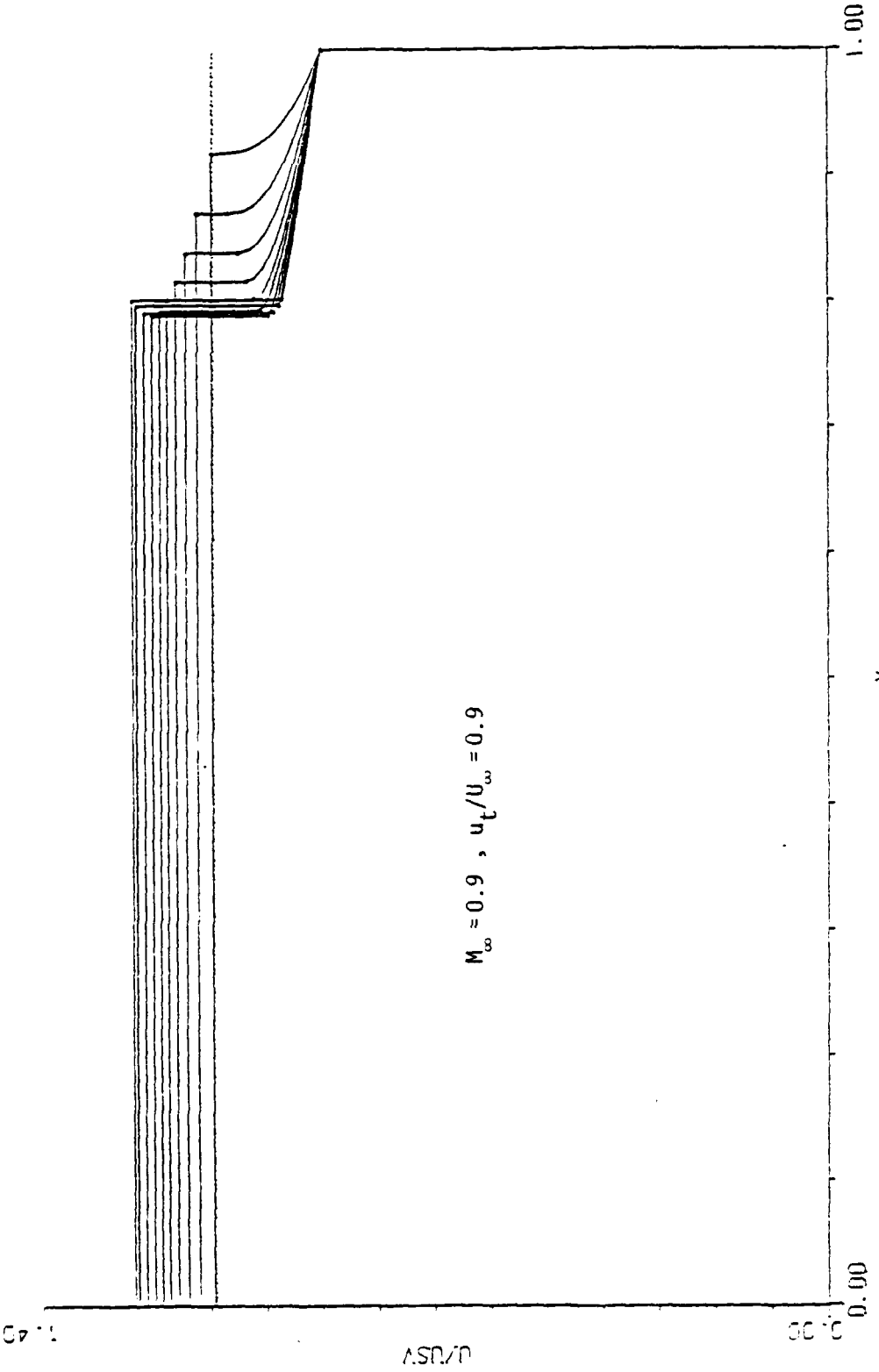

Figure 17. A Family of Shock Solutions for Given Values of M_∞ and u_t/U_∞

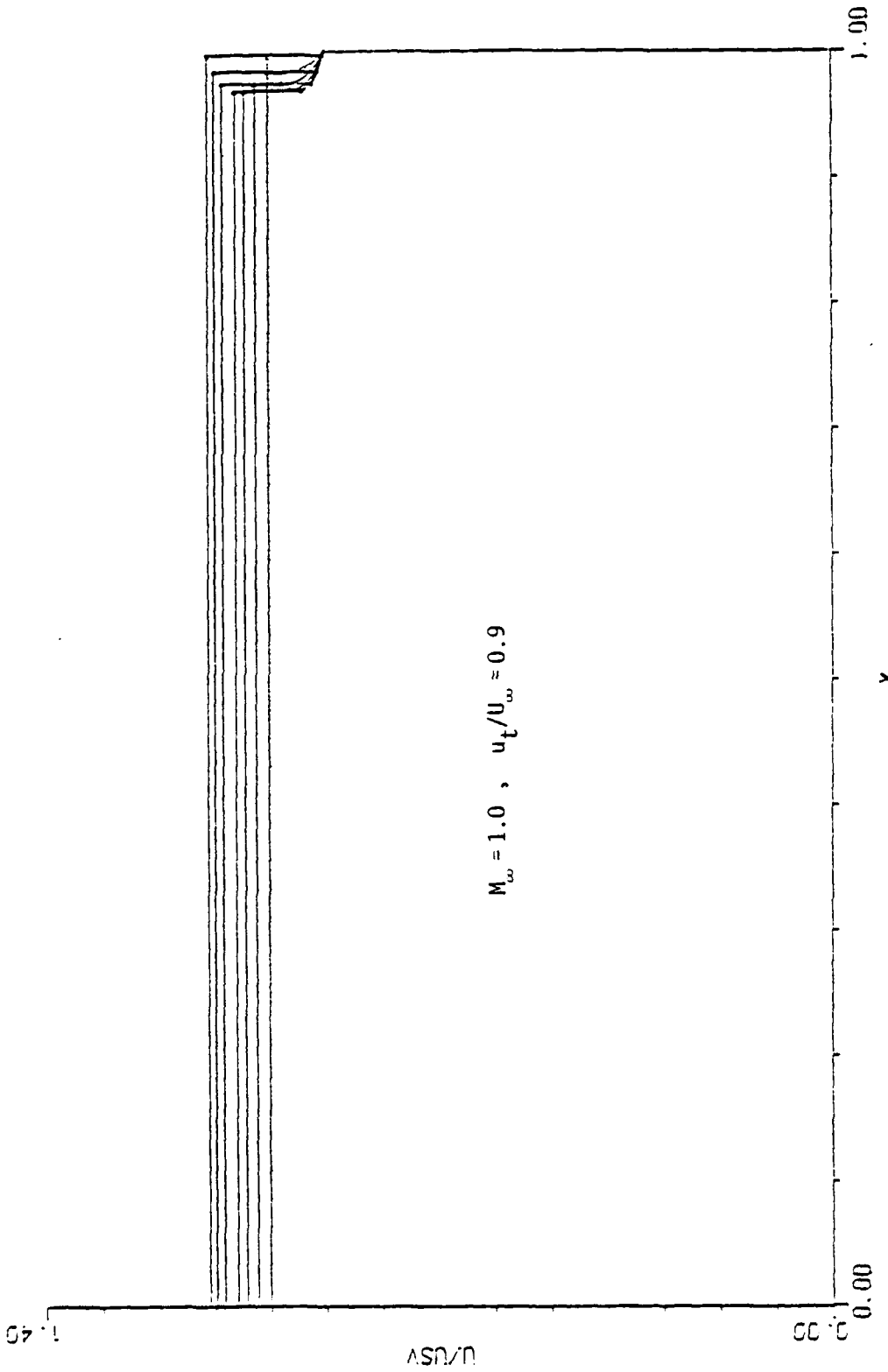

Figure 18. A Family of Shock Solutions for Given Values of M_∞ and u_t/U_∞

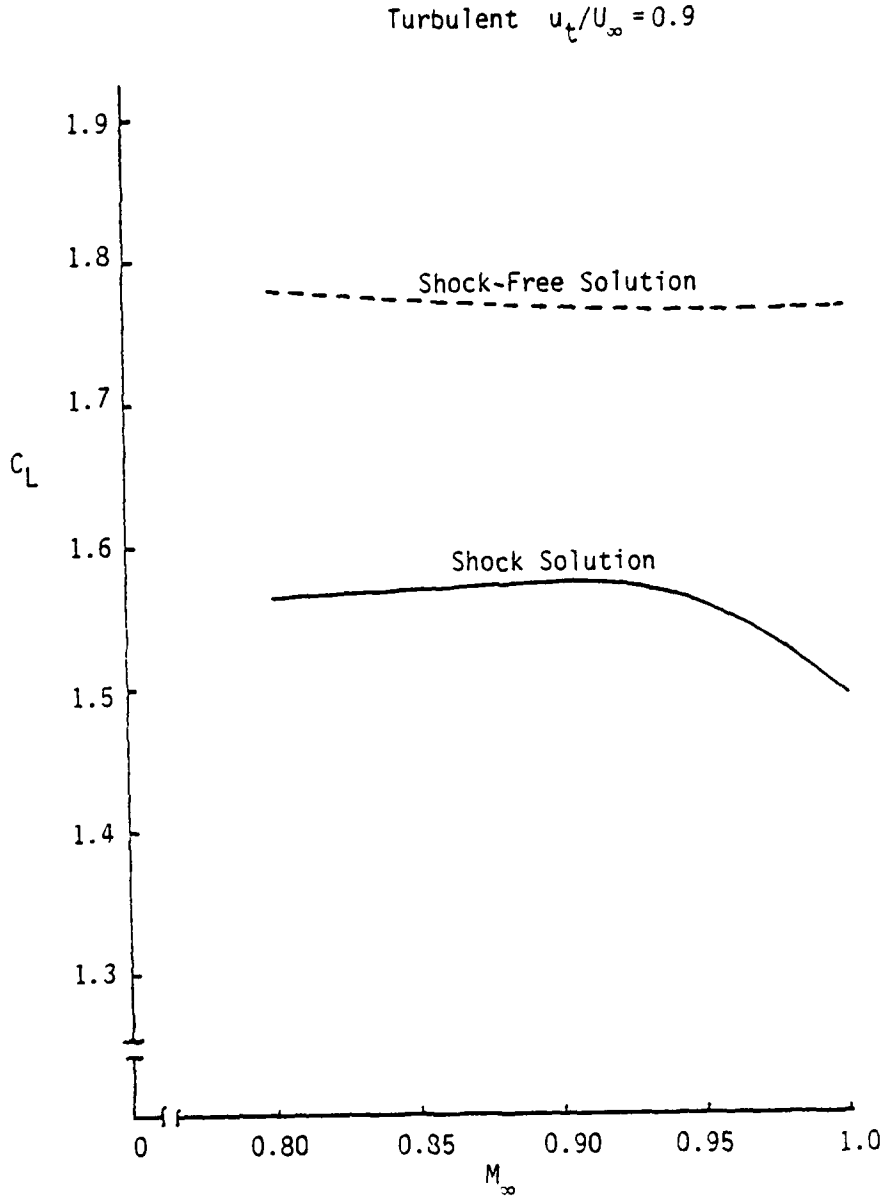

Figure 19. Maximum C_L With and Without Shock

APPENDIX A

Development of a Compressible Separation Criterion for Turbulent Boundary Layers

Inner Field Development

The inner field region corresponds to the flow within the turbulent boundary layer near the wall surface. Within this region, we assume fully turbulent flow and use the Prandtl mixing length hypothesis to represent the shear stress with $\ell=\kappa y$ where κ is von Karman's constant and y is the local measure of transverse distance along the surface. The shear stress is given by the expression

$$\tau = \rho\kappa^2 y^2 \left(\frac{\partial u}{\partial y}\right)^2 \qquad \text{(A-1)}$$

By integrating the boundary layer equations from the wall outward to some point y, which is also near the wall, we obtain

$$\tau = \tau_w + y \frac{dp}{ds} \quad ; \quad p = p(s) \qquad \text{(A-2)}$$

where the external pressure gradient has been assumed to be impressed upon the boundary layer.

Equating τ's in expressions (A-1) and (A-2) gives the flow speed gradient at a point y_* where the two expressions for τ are equal. That is,

$$\left(\frac{\partial u}{\partial y}\right)_*^2 = \left[\frac{\frac{dp}{ds}}{\rho\kappa^2}\right] y_*^{-1} + \frac{\tau_w}{\rho\kappa^2} y_*^{-2} \qquad \text{(A-3)}$$

Assuming separation occurs when τ_w vanishes, expression (A-3) can be viewed as a partial differential equation for the flow speed in a region of sufficiently small y . That is, setting $\tau_w = 0$ in the previous equation, gives

$$\left(\frac{\rho}{\rho_w}\right)^{1/2} \frac{\partial \zeta}{\partial y} = \Lambda\, y^{-1/2} \quad \text{when } \tau_w = 0 \qquad \text{(A-4)}$$

where

$\zeta \equiv u/u_o$, a speed ratio scaled with the reference speed u_o.

$\Lambda \equiv \left(\rho_w^{-1} \kappa^{-2} u_o^{-2} \frac{dp}{ds}\right)^{1/2}$, a pressure gradient coefficient (varying with location s)

Before equation (A-4) can be integrated, we must determine how the density ratio ρ/ρ_w depends on the streamwise speed. For a perfect gas, the density ratio is related to the temperature ratio by

$$\frac{\rho}{\rho_w} = \frac{T_w}{T} \tag{A-5}$$

From Crocco's relationship (see Reference [9], page 144), we have that

$$\frac{T}{T_w} = (1 + B_1 \zeta - A^2 \zeta^2) \tag{A-6}$$

where

$$\left.\begin{aligned} A^2 &\equiv \frac{[(\gamma-1)/2]}{T_w/T_e} M_e^2 \\ B_1 &\equiv \frac{1 + [(\gamma-1)/2] M_e^2}{T_w/T_e} - 1 \end{aligned}\right\} \tag{A-7}$$

Therefore, combining equations (A-4) - (A-7) gives

$$\frac{\frac{\partial \zeta}{\partial y}}{(1+B_1\zeta-A^2\zeta^2)^{1/2}} = \Lambda\, y^{-1/2} \qquad \text{when } \tau_w = 0 \tag{A-8}$$

This equation can be integrated as an ordinary differential equation since s enters only as a parameter through the terms A, B_1 and Λ. Integrating from the wall outward the solving for ζ as a function of y yields

$$\zeta = \xi \sin (2\Lambda A \sqrt{y} - \epsilon) + \eta \tag{A-9}$$

where

$$\left.\begin{aligned} \xi &\equiv \left(4A^2 + B_1^2\right)^{1/2}/2A^2 \\ n &\equiv B_1/2A^2 \\ \varepsilon &\equiv \sin^{-1}\left[B_1/\left(4A^2 + B_1^2\right)^{1/2}\right] \end{aligned}\right\} \qquad \text{(A-10)}$$

To approximate the flow speed ratio near the wall at separation, we expand the sine function appearing in equation (A-9) using the trigonometric relation for the sine of the difference of two angles together with the series expansions for the sine and cosine of small angles. Neglecting higher order terms in the expansion, we obtain

$$\zeta = 2\Lambda\sqrt{y}\left[1 + \frac{\Lambda}{2}B_1\sqrt{y} + O(y)\right] \; ; \quad \begin{cases} y << 1 \\ \\ \tau_w = 0 \end{cases} \qquad \text{(A-11)}$$

Notice that the flow speed tends to zero in a square root fashion at separation as the wall is approached. The leading order term is similar to the incompressible result (suitably modified by the compressible pressure gradient term in Λ) and the next term contains a heat transfer contribution and a Mach number effect (see equation (A-7)). The streamwise speed gradient at separation is obtained by differentiation of equation (A-11). Hence,

$$\frac{\partial\zeta}{\partial y} = \Lambda\, y^{-1/2}\left[1 + \Lambda B_1 y^{1/2} + O(y)\right] \; ; \quad \begin{cases} y << 1 \\ \\ \tau_w = 0 \end{cases} \qquad \text{(A-12)}$$

and the slope of the flow speed is infinite at separation, tending there as the inverse square root of the transverse distance.

To complete the near field specification, we require the stream function in the boundary layer. A suitable definition of the stream function for compressible flow is

$$\psi = u_o \int_o^y \left(\frac{\rho}{\rho_w}\right)\zeta dy \tag{A-13}$$

But for $y << 1$ (which implies that $\zeta << 1$ from equation (A-11))

$$\frac{\rho}{\rho_w} = \left(1 + B_1\zeta - A^2\zeta^2\right)^{-1} \approx 1 - B_1\zeta + O(\zeta^2) \tag{A-14}$$

Substituting equation (A-11) into equation (A-14) and the resulting expression into equation (A-13) gives, upon integration

$$\psi = \frac{4}{3} u_o \Lambda y^{3/2}\left[1 + \frac{3}{2}\Lambda B_1 y^{1/2} + O(y)\right] \; ; \quad \begin{cases} y << 1 \\ \tau_w = 0 \end{cases} \tag{A-15}$$

Later in the development we will equate certain inner and outer physical quantities in an overlapping region to obtain the separation criterion. The technique is not an "asymptotic matching" in the strict sense, but rather falls into the category of a "patching" approach. The procedure is not unique. Nevertheless, we follow Stratford in this development in view of the success he obtained. In so doing, we require the limiting forms (for $y << 1$ and $\tau_w = 0$) of the quantities $\psi\left(\frac{\partial\zeta}{\partial y}\right)^3$ and $\zeta^2/\left(\psi\,\frac{\partial\zeta}{\partial y}\right)$.

These are readily obtained from equations (A-11), (A-12) and (A-15). They are

$$\psi\left(\frac{\partial \zeta}{\partial y}\right)^3 = \frac{4}{3} u_o \Lambda^4 \left[1 + \frac{3}{2} \Lambda B_1 \sqrt{y} + O(y)\right] \; ; \; \begin{cases} y << 1 \\ \\ \tau_w = 0 \end{cases} \tag{A-16}$$

$$\frac{\zeta^2}{\psi\left(\frac{\partial \zeta}{\partial y}\right)} = \frac{3}{u_o} \left[1 + \frac{3}{2} \Lambda B_1 \sqrt{y} + O(y)\right] \; ; \; \begin{cases} y << 1 \\ \\ \tau_w = 0 \end{cases} \tag{A-17}$$

The physical significance of these quantities is unclear. However, it is perhaps interesting that equations (A-16) and (A-17) have the expressions in brackets in common - at least to O(y). The ratios were originally chosen (most likely) to clear the y dependence from the leading order terms.

Outer Field Development

The outer field is considered to be the region in the turbulent boundary layer, well removed from the surface of the body. If a pressure rise did not exist in this region, the velocity profile would be similar to that along a turbulent flat plate. The total pressure loss can be calculated for such a case. For the real case of a pressure rise we make the assumption that the loss of total pressure along a stream line is independent of the pressure rise. This assumption is supported by experimental results. (See Reference [3], Grabowski *et al.*). If the pressure rise is severe, the assumption should be even more reliable since it will produce the effect of an instantaneous change of flow conditions over a short spatial duration and for such a change the effects of dissipation are negligible. As a consequence, we assume that the pressure loss along the stream line in the actual case is the same as on a corresponding stream line in the turbulent flat plate case where the pressure is constant.

In the outer region, we assume the Bernoulli equation, applied along a stream line, holds true in the form:

$$\frac{u^2}{2} + \int \frac{dp}{\rho} = f(\psi) \quad , \quad \text{along } \psi \geq \psi_i \tag{A-18}$$

where ψ_i denotes a limiting stream line on the inner periphery of the outer region. (ψ_i is unknown and can be found as part of the solution.)

In this outer region we assume the flow is well represented by an adiabatic, inviscid and nonconducting fluid flow. Such a flow is isentropic and is described by the isentropic relation

$$\frac{p}{p_0} = \left(\frac{\rho}{\rho_0}\right)^{\gamma} = \left(\frac{T}{T_0}\right)^{\gamma/(\gamma-1)} \tag{A-19}$$

Substituting Equation (A-19) into the Bernoulli equation yields

$$\frac{u^2}{2} + \frac{\gamma}{(\gamma-1)} \frac{p_0}{\rho_0} (p/p_0)^{(\gamma-1)/\gamma} = f(\psi) \quad ; \quad \psi \geq \psi_i \tag{A-20}$$

Now assume that far from the wall a comparison velocity profile $u_c \equiv u_c(s,\psi)$ exits (subscript c denotes the comparison flow) and is a reasonably accurate representation of the flow field in the outer boundary layer. (Notice that the y dependence enters implicitly by way of ψ.) At some point $s = s_0$ corresponding to the beginning of the pressure recovery (the reference point), we have that

$$\left.\begin{aligned} u(s_0,\psi) &= u_c(s_0,\psi) \\ p &= p_0 \end{aligned}\right\} \tag{A-21}$$

The relations appearing in equation (A-21) are used to evaluate the Bernoulli 'constant' of equation (A-20). Dividing equation (A-20) by $u_0^2/2$ results in

$$\left.\begin{aligned} \zeta^2 &= \zeta_c^2 - C_p^*(s) \\ \text{where} \quad C_p^*(s) &\equiv \frac{\gamma}{(\gamma-1)} \frac{p_o}{\frac{1}{2}\rho_o u_o^2}\left[\left(\frac{p}{p_o}\right)^{\frac{\gamma-1}{\gamma}} - 1\right] \\ \zeta_c &\equiv \frac{u_c(s,\psi)}{u_o} \\ \zeta &\equiv \frac{u(s,\psi)}{u_o} \end{aligned}\right\} \qquad \text{(A-22)}$$

Taking the partial derivative with respect to ψ of the Bernoulli integral (A-22) gives

$$\zeta \frac{\partial \zeta}{\partial \psi} = \zeta_c \frac{\partial \zeta_c}{\partial \psi} \qquad \text{(A-23)}$$

From the definition of the stream function given by equation (A-13) we have that

$$\frac{\partial \psi}{\partial y} = u_o\left(\frac{\rho}{\rho_w}\right)\zeta \quad ; \qquad \left(\frac{\partial \psi}{\partial y}\right)_c = u_o \left(\frac{\rho}{\rho_w}\right)_c \zeta_c$$

Therefore,

$$\left.\begin{aligned} \frac{\partial \zeta}{\partial y} &= \frac{\partial \psi}{\partial y}\frac{\partial \zeta}{\partial \psi} = u_o\left(\frac{\rho}{\rho_w}\right)\zeta \frac{\partial \zeta}{\partial \psi} \\ \frac{\partial \zeta_c}{\partial y} &= \left(\frac{\partial \psi}{\partial y}\right)_c \frac{\partial \zeta_c}{\partial y} = u_o \left(\frac{\rho}{\rho_w}\right)_c \zeta_c \frac{\partial \zeta_c}{\partial \psi} \end{aligned}\right\} \qquad \text{(A-24)}$$

Comparing Equations (A-23) and (A-24) and assuming $(\rho/\rho_w)_c = (\rho/\rho_w)$, we obtain

$$\frac{\partial \zeta}{\partial y} = \frac{\partial \zeta_c}{\partial y} \qquad \text{(A-25)}$$

Using Crocco's relationship for the comparison flow we obtain

$$\left(\frac{\rho}{\rho_w}\right)_c = \frac{1}{\left(1 + B_1\zeta_c - A^2\zeta_c^2\right)} \tag{A-26}$$

$$\psi \tilde{=} u_o \int_o^y \frac{\zeta_c}{\left(1 + B_1\zeta_c - A^2\zeta_c^2\right)}\, dy \tag{A-27}$$

$$\frac{\partial\zeta}{\partial y} = \frac{\partial\zeta_c}{\partial y} \tag{A-28}$$

and from equation (A-22)

$$\zeta^2 = \zeta_c^2 - C_p^*(s) \tag{A-29}$$

Equations (A-29), (A-28) and (A-27), representative of the outer field, are comparable to the inner field equations (A-11), (A-12) and (A-15), respectively.

We now assume the following power law expression* for the comparison flow:

$$\zeta_c = \lambda y^m \; ; \quad \lambda \equiv k_1/\theta^m \tag{A-30}$$

where the power m of y and the coefficient λ (expressed in terms of a constant k_1 determined from experimental data and the momentum thickness θ) are given by turbulent flat plate boundary layer experiment. Experimental evidence exists showing m = 1/7 fits data well even for a Mach number as great as 2.4.

Equation (A-30) is to be substituted into equations for ψ, ζ and $\partial\zeta/\partial y$ (previously given). The immediate objective is to develop the far field patching conditions. In so doing, we will push the far field results to

* Other velocity profiles can be chosen, for example, Cole's law of the wall/law of the wake. However, the assumptions inherent in this Stratford type development do not warrant such sophistication.

the limit of small y. Patching will then provide y at the join ($y=y_j$) and a relationship of the actual velocity profile to the comparison profile. Hence, for small y

$$\left.\begin{aligned} &\frac{\partial \zeta}{\partial y} \approx \frac{\partial \zeta_c}{\partial y} = \lambda\, m\, y^{m-1} \quad ; \quad y << 1 \\ &\psi \approx u_o \int_o^y \zeta_c(1-B_1\zeta_c)dy \approx u_o \lambda \frac{y^{m+1}}{(m+1)}\left[1-B_1\lambda\frac{(m+1)}{(2m+1)}\,y^m\right];\ y << 1 \end{aligned}\right\} \quad (A\text{-}31)$$

The patching conditions are readily obtained from these expressions. They are

$$\psi\left(\frac{\partial \zeta}{\partial y}\right)^3 \approx u_o \lambda^4 \frac{m^3}{(m-1)}\, y^{4m-2}\left[1 - \frac{m+1}{2m+1}\, B_1 \lambda\, y^m\right] \quad (A\text{-}32)$$

$$\frac{\zeta^2}{\left(\psi \frac{\partial \zeta}{\partial y}\right)} \approx \frac{\zeta^2}{\zeta_c^2}\frac{(m+1)}{m}\frac{1}{u_o}\left[1 + B_1\lambda\frac{(m+1)}{(2m+1)}\, y^m\right] \quad (A\text{-}33)$$

Notice that the expresions in brackets above are not identical, as they were found to be for the similar conditions obtained in the inner field. This disparity arises because the approximation for the stream function, flow speed and transverse flow speed gradient (using the comparison profile) become weak for $y << 1$. However, to leading order in y, this disparity does not upset the approach we are using. It would, however, affect matters if a higher order development were pursued. In that case, a better representation of the velocity profile in the outer boundary layer for small y would be warranted.

Furthermore, it should be noted that the relationship between ζ, ζ_c and C_p^* (equation (A-29)) was not used in obtaining equation (A-33). After equating the near field and far field results, equation (A-29) provides the separation criterion.

Patching

To find y at the patching locating ($y=y_j$) we equate the coefficients of equations (A-16) and (A-32) and obtain

$$\frac{4}{3}\Lambda^4 = \lambda^4 \frac{m^3}{(m+1)} y_j^{4m-2} \tag{A-34}$$

Solving this expression for y_j/θ (see equation (A-30)) gives

$$(y_j/\theta)^{2-4m} = \frac{3}{4}\frac{m^4}{(m+1)}\frac{k_1^4}{\theta^2\Lambda^4} \tag{A-35}$$

To find the relationship between the actual velocity profile and the comparison profile at the patching location, we equate coefficients of equations (A-17) and (A-33) and obtain*

$$\left(\frac{\zeta}{\zeta_c}\right)_j^2 = \frac{3m}{(m+1)} \tag{A-36}$$

---

* Notice that $C_p^* = \zeta_c^2(1-\zeta^2/\zeta_c^2) = \lambda^2 y^{2m}[1-3m/(m+1)]$ +

$$C_p^* \leq (1-2m)/(1+m) \equiv (n-2)/(n+1) \; ; \; m \equiv 1/n$$

Separation Criterion

Equations (A-29), (A-35) and (A-36) contain the essential results of the analysis thus far. Since we seek a separation criterion in terms of C_p^*, it is necessary to express dp/ds appearing in the Λ expression (see Λ definition occurring after equation (A-4)) in terms of C_p^*.

From equation (A-22) and the isentropic gas relationship (A-19)

$$\frac{dp}{ds} = \left(\frac{1}{2}\rho_e u_o^2\right)\frac{dC_p^*}{ds} \tag{A-37}$$

It should be noticed that the density ρ_e appears in the pressure gradient expression rather than the reference density ρ_o or ρ_w.

Consequently, the term $\Lambda^4\theta^2$ in Equation (A-35) becomes

$$\Lambda^4\theta^2 = \frac{1}{4}\left(\frac{\rho_e}{\rho_w}\right)^2 \frac{1}{\kappa^4}\left(\theta\frac{dC_p^*}{ds}\right)^2 \tag{A-38}$$

and equation (A-35) becomes

$$(y_j/\theta)^{2-4m} = \left(\frac{3m^3}{m+1}\right)\left(\frac{\rho_w}{\rho_e}\right)^2 (\kappa k_1)^4 \left(\theta\frac{dC_p^*}{ds}\right)^{-2} \tag{A-39}$$

The density ratio can be expressed as

$$\frac{\rho_w}{\rho_e} = \frac{1}{\left(1+B_1-A^2\right)} = \frac{T_e}{T_w} \tag{A-40}$$

With the additional assumption that the wall is an adiabatic wall $(T_w \equiv T_{aw})$ then,

$$\left(\frac{\rho_w}{\rho_e}\right)_a = \left[1 + r\frac{(\gamma-1)}{2}M_e^2\right]^{-1} \tag{A-41}$$

and since the local inviscid Mach number varies along the airfoil surface the quantity $(\rho_w/\rho_e)_a$ is a function of s.

The recovery factor r is approximately equal to 0.9 (see Reference [9]). Equation (A-39) can be written as

$$(y_j/\theta)^{\frac{1-2m}{2}} = \kappa k_1 \left(\frac{3m^3}{m+1}\right)^{1/4} \left(\frac{\rho_w}{\rho_e}\right)_a^{1/2} \left(\theta \frac{dC_p^*}{ds}\right)^{-1/2} \qquad \text{(A-42)}$$

Combining Equations (A-29), (A-30) and (A-36) and solving for $(y_j/\theta)^{2m}$ gives

$$(y_j/\theta)^{2m} = \frac{2\, C_p^*}{2\, k_1^2\left[1 - \frac{3m}{(m+1)}\right]} \quad ; \quad \frac{3m}{(m+1)} < 1 \qquad \text{(A-43)}$$

Eliminating (y_j/θ) from equations (A-42) and (A-43) gives the separation criterion. Letting m = 1/n recovers Stratford's form of the criterion. That is,

$$\left[C_p^*\right]^{\frac{1}{4}(n-2)} \left(\theta \frac{dC_p^*}{ds}\right)^{1/2} = \kappa k_1^{\frac{n}{2}} \left[\frac{3}{n^2(n+1)}\right]^{1/4} \left(\frac{n-2}{n+1}\right)^{\frac{1}{4}(n-2)} \left(\frac{\rho_w}{\rho_e}\right)_a^{1/2} \qquad \text{(A-44)}$$

where $0 \leq C_p^* \leq (n-2)/(n+1)$ is required (see footnote on page 66).

Compressible Momentum Thickness

Stratford expresses θ as a function of local Reynolds number R_s and s for the incompressible case. One way to proceed is to look at the local skin friction coefficient c_f vs. M_e curves as in Clutter's report [11]. These are based on the Van Driest II formula and are considered state of the technology.

One starts with the momentum integral equation for a flat-plate boundary layer

$$\frac{d\theta}{ds} = \frac{\tau_w}{\rho_o u_o^2} \qquad \text{(A-45)}$$

where

$$\tau_w = c_f \left(\frac{1}{2} \rho_o u_o^2\right)$$

If a power law form for c_f is assumed

$$c_f = a\, R_s^b$$

then equation (A-45) can be integrated to give θ with the desired functional dependence. For Mach numbers in the range 0 to 2 and Reynolds numbers in the range 10^6 - 10^7 the variation of the constants a,b were found [4] to be about ten percent. Considering the approximate nature of the Stratford method to begin with, we take a,b to be values found when M_e is near unity. That is,

$$a \equiv 0.036$$
$$b \equiv -1/6$$

Then

$$\theta = 0.022\, s\, R_s^{-1/6}$$

The separation criterion can be written, therefore, as

$$\left.\begin{aligned} \left(C_p^*\right)^{\frac{1}{4}(n-2)} \left(s\,\frac{dC_p^*}{ds}\right)^{1/2} &= g(n)\left(\frac{\rho_w}{\rho_e}\right)_a^{1/2} \left(R_s \cdot 10^{-6}\right)^{1/12}, \quad 0 \le C_p^* \le \frac{n-2}{n+1} \\ g(n) &\equiv 21.32 \left(\frac{3}{n^2(n+1)}\right)^{1/4} \left(\frac{n-2}{n+1}\right)^{\frac{n-2}{4}} \kappa (k_1)^{n/2} \end{aligned}\right\} \quad \text{(A-46)}$$

This is the form of the separation criterion reported in the introduction to this section. The density ratio on the right hand side is given by equation (A-41).

From Reference [8] (Schlichting, pg. 674, giving measurements on a flat plate at zero incidence to the flow) we find that the 1/7th power law fitting experimental data quite well even when Mach number equals 2.4. In this case, the empirical constant k_1 is

$$k_1 = 0.683$$

which will be assumed to remain valid throughout this development for other values of n, as well.

Stratford [1] expresses his separation criterion in terms of the pressure coefficient $\bar{C}_p$ referenced to the dynamic head at the peak velocity point. That is,

$$\bar{C}_p \equiv \frac{p_o}{\frac{1}{2}\rho_o u_o^2}\left(\frac{p}{p_o} - 1\right) \qquad \text{(A-47)}$$

C_p^* is related to $\bar{C}_p$ by

$$\left.\begin{aligned} C_p^* &= \frac{\gamma}{(\gamma-1)} \frac{p_o}{\frac{1}{2}\rho_o u_o^2}\left[\left(1 + \frac{\frac{1}{2}\rho_o u_o^2 \bar{C}_p}{p_o}\right)^{\frac{\gamma-1}{\gamma}} - 1\right] \\ C_p^* &= \frac{2}{(\gamma-1)} M_o^{-2}\left[\left(1 + \frac{\gamma}{2} M_o^2 \bar{C}_p\right)^{\frac{\gamma-1}{\gamma}} - 1\right] \end{aligned}\right\} \qquad \text{(A-48)}$$

From this last expression it can be seen that $C_p^* \to \bar{C}_p$ as $M_o \to 0$.

Another way of expressing C_p^* is in terms of the flow speed ratio u_e/u_o. From Reference [12] (page 55) we have that

$$\frac{p}{p_o} = \frac{\gamma M_o^2}{2} \bar{C}_p + 1$$

$$\bar{C}_p = \frac{2}{\gamma M_o^2}\left[\left\{1 + \frac{\gamma-1}{2} M_o^2 \left(1 - \frac{u_e^2}{u_o^2}\right)\right\}^{\frac{\gamma}{\gamma-1}} - 1\right] \qquad \text{(A-49)}$$

Combining this last result with the last of equation (A-48) gives

$$C_p^* = \left[1 - \left(\frac{u_e}{u_o}\right)^2\right] \qquad \text{(A-50)}$$

Since the pressure coefficient is determined from conditions prevailing external to the boundary layer (the inviscid solution), the previous expression for C_p^* could have been deduced immediately from the Bernoulli equation (A-22). In that expression, $\zeta_c = 1$ along the edge of the boundary layer.

APPENDIX B

Derivation of the Compressible Stratford Flows

Compressible Stratford Flows

The density ratio on the right hand side of equation (A-46) depends on the boundary layer edge Mach number M_e, as given by equation (A-41). From the Bernoulli equation, the edge Mach number is related to C_p^* and the peak Mach number M_o by

$$M_e^2 = (1 - C_p^*)\, M_o^2 \Big/ \left(1 + \frac{\gamma-1}{2} M_o^2\, C_p^*\right) \tag{B-1}$$

Combining equations (B-1) and (A-41) gives

$$\left(\frac{\rho_w}{\rho_e}\right)_a = \frac{1 + \frac{(\gamma-1)}{2} M_o^2\, C_p^*}{\left[1 + r\,\frac{(\gamma-1)}{2} M_o^2\right] + \left[(1-r)\,\frac{(\gamma-1)}{2} M_o^2\, C_p^*\right]} \tag{B-2}$$

To a good approximation, equation (B-2) can be expanded using the binomial series to give

$$\left.\begin{aligned} \left(\frac{\rho_w}{\rho_e}\right)_a &\approx \frac{1}{\left[1 + r\,\frac{(\gamma-1)}{2} M_o^2\right]}\; 1 + \mu\, C_p^* \\ \text{where} \qquad \mu &\equiv r\left[\frac{1 + \frac{\gamma-1}{2} M_o^2}{1 + r\,\frac{\gamma-1}{2} M_o^2}\right] \frac{(\gamma-1)}{2} M_o^2 \end{aligned}\right\} \tag{B-3}$$

Specializing to $n = 6$, equation (A-46) can be integrated using equation (B-3) to yield

$$C_p^* \approx B\left[\left(\frac{s}{s_o}\right)^{1/6} - 1\right]^{1/3}\left[1 + \frac{1}{4}\,\mu B\left\{\left(\frac{s}{s_o}\right)^{1/6} - 1\right\}^{1/3} + \ldots\right] \;;\; C_p^* \leq \frac{4}{7} \tag{B-4}$$

where

$$B^3 \equiv \frac{18 g^2(6)\left(R_{s_o} \cdot 10^{-6}\right)^{1/6}}{1 + r\,\frac{(\gamma-1)}{2} M_o^2} \;;\; g(6) \approx 0.52 \tag{B-5}$$

The speed ratio u_e/u_o can be obtained from equation (B-4) since

$$u_e/u_o = (1 - C_p^*)^{1/2} \quad ; \sqrt{\frac{3}{7}} \leq \frac{u_e}{u_o} \leq 1 \tag{B-6}$$

If s_c denotes the point where $C_p^* = 4/7$, then from equation (B-4)

$$\frac{s_c}{s_o} = \left[1 + \frac{4}{7B}^{3} (1 - \frac{\mu}{7})\right]^6 \tag{B-7}$$

To obtain an expression for $C_p^*(s)$ for values greater than 4/7, use is made of the momentum integral in the streamwise direction which can be written as

$$\rho_e u_e^2 \theta' + \rho_e \theta u_e u_e' \left(2 + H - M_e^2\right) = \tau_w \tag{B-8}$$

where

θ is the momentum thickness

H is the boundary layer shape factor*

τ_w is the wall shear stress

and 'prime' denotes differentiation with respect to s.

Setting the wall shear stress to zero and assuming the shape factor is constant, equation (B-8) integrates to

$$\rho_e \theta = \alpha_1 / (1 - C_p^*)^{1+H/2} \tag{B-9}$$

where α_1 is the constant of integration.

---

* For turbulent flow, separation is assumed to occur for values of H between 1.8 and 2.4.

When $C_p^* = 4/7$ the inner region of the boundary layer (as described in Appendix A in the section on the Inner Field Development) extends all the way to the edge of the boundary layer. In the decelerated flow region where $(u_e/u_o \leq \sqrt{3/7})$, we assume that the speed ratio can reasonably be represented by the first term in the expansion given by equation (A-11) evaluated at $y = y_e = \delta$. That is,

$$\left(\frac{u_e}{u_o}\right)^2 \equiv 1 - C_p^* = 4\,\Lambda^2\delta$$

But, from equation (A-38)

$$\Lambda^2 = \frac{1}{2}\frac{\rho_e}{\rho_w}\frac{1}{\kappa^2}\left(\frac{dC_p^*}{ds}\right)$$

so that

$$\frac{dC_p^*}{ds} = \frac{\kappa^2}{2}\left(\frac{\rho_w}{\rho_e}\right)\frac{(1 - C_p^*)}{\delta} \qquad \text{(B-10)}$$

If it is assumed δ remains proportional to the momentum thickness θ for $s \geq s_c$ (a similarity solution) then equations (B-9) and (B-10) can be combined to give

$$\frac{d(1-C_p^*)}{ds} = \alpha_2\frac{(1-C_p^*)}{\rho_e\theta} = \frac{\alpha_2}{\alpha_1}(1-C_p^*)^{2+\frac{H}{2}} \qquad \text{(B-11)}$$

where α_2 is the constant of propportionality relating θ to δ (i.e., $\theta = \alpha_2\delta$). Integrating equation (A-13) and selecting $H = 2$ (the value assumed by Stratford) yields

$$C_p^*(s) = 1 - (\alpha_3 s + \alpha_4)^{-1/2} \quad ; \quad s \geq s_c \qquad \text{(B-12)}$$

where the constants α_3, α_4 are determined by requiring that C_p^* and dC_p^*/ds (from equation (B-12) match at $s = s_c$ with the C_p^* and dC_p^*/ds expressions obtained from the separation criterion. This process leads

to

$$\left.\begin{aligned} \alpha_3 &= \frac{343}{243}\frac{B}{s_c}\left(\frac{s_c}{s_o}\right)^{1/6}\left[\left(\frac{s_c}{s_o}\right)^{1/6} - 1\right]^{-2/3}\left[1 + \frac{B}{2}\mu\left\{\left(\frac{s_c}{s_o}\right)^{1/6} - 1\right\}^{1/3}\right] \\ \alpha_4 &= \frac{49}{9} - \alpha_3 s_c \end{aligned}\right\} \quad \text{(B-13)}$$

APPENDIX C

Shock Considerations

Momentum Thickness Aft of a Normal Shock

Consider the development of a boundary layer along a flat plate. Suppose at some point s_s along the plate a normal shock wave occurs. The shock wave interacts with the boundary layer and modifies its velocity profile. As a consequence, the momentum thickness is substantially changed through the shock.

Figure C-1 presents an illustration of a flat plate boundary layer in the vicinity of a normal shock wave. Our immediate intent is to derive an expression for the momentum thickness θ at station $s = s_s + \varepsilon$ where s_s denotes the shock location and ε is a small value measuring the effective distance over which the shock and turbulent boundary layer interact. The expression can be developed by applying the principles of conservation of mass and momentum and the normal shock relations to the control volume shown in Figure C-1. The control volume is rectangular having a length s (measured from the plate's leading edge) and a height $\delta(s)$ equal to the boundary layer thickness at station s. The conservation of mass (in integral form) states:

$$\int_0^{\delta(s)} [\rho_o u_o - \rho u]\, dy = \int_0^{s_s} \rho v d\xi + \int_{s_s}^{s} \rho v d\xi \qquad (C\text{-}1)$$

where ρ is the density

u is the velocity component in the freestream direction, s

v is the transverse velocity component.

Quantities with subscript "o" denote freestream values.

Applying the integral form of the conservation of momentum (s-component) to the control volume gives

$$F_s \equiv \int_0^{\delta(s)} (p_o - p_1) dy - \int_0^{s} \tau_w(s) ds$$

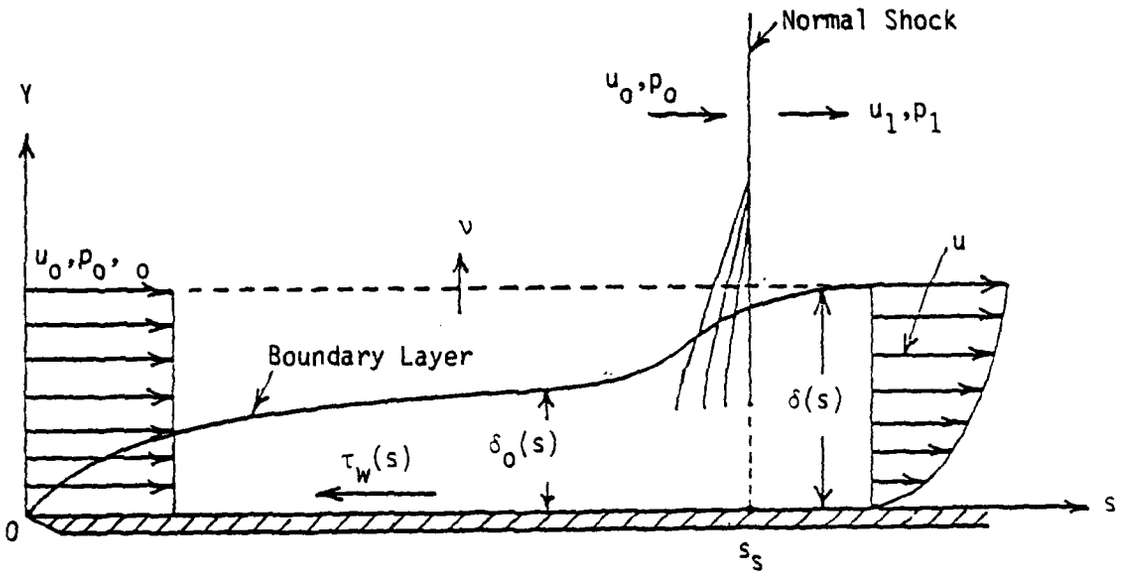

Figure C-1. Interaction Between a Flat Plate Boundary Layer and a Normal SHock

(C-2)

$$= \int_0^{\delta(s)} (\rho u^2 - \rho_0 u_0^2)\,dy + \int_0^{s_s} \rho u_0 v\,ds + \int_{s_s}^{s} \rho u_1 v\,ds$$

where p_1 is pressure aft of the shock

τ_w is the shear stress acting along the wall

u_1 is the s-component of the fluid speed aft of the shock and external to the boundary layer.

The pressure p_1 and the velocity component u_1 are related to the corresponding quantities p_0, u_0 through the normal shock relations. That is,

$$\frac{u_1}{u_0} = \frac{(\gamma-1)\,M_0^2 + 2}{(\gamma+1)\,M_0^2} \qquad (C\text{-}3)$$

$$\frac{p_1}{p_0} = 1 + \frac{2\gamma}{(\gamma+1)}\,(M_0^2 - 1)$$

where $\gamma = 1.4$ is the adiabatic index and M_0 is the freestream Mach number.

Combining equations (C-1) and (C-2) gives

$$\int_0^{\delta(s)} \rho u(u_0 - u)\,dy - (u_1 - u_0)\int_{s_s}^{s} \rho v\,ds = \int_0^{\delta(s)} (p_1 - p_0)\,dy + \int_0^{s} \tau_w(s)\,ds \qquad (C\text{-}4)$$

To a leading order approximation, we can estimate the momentum thickness aft of the shock by assuming the interaction region shrinks to zero and causes a step change in the momentum thickness (see Equation (C-7) for definition of θ) at the shock location s_s (see Figure C-2). That is, substituting $s = s_s + \varepsilon$ into equation (C-4) and taking the limit as $\varepsilon \to 0^+$ gives:

$$u_0 \int_0^{\delta(s^+)} \rho u \left(1 - \frac{u}{u_0}\right) dy = \int_0^{\delta(s^+)} (p_1 - p_0)\,dy + \int_0^{s^+} \tau_w(s)\,ds \qquad (C\text{-}5)$$

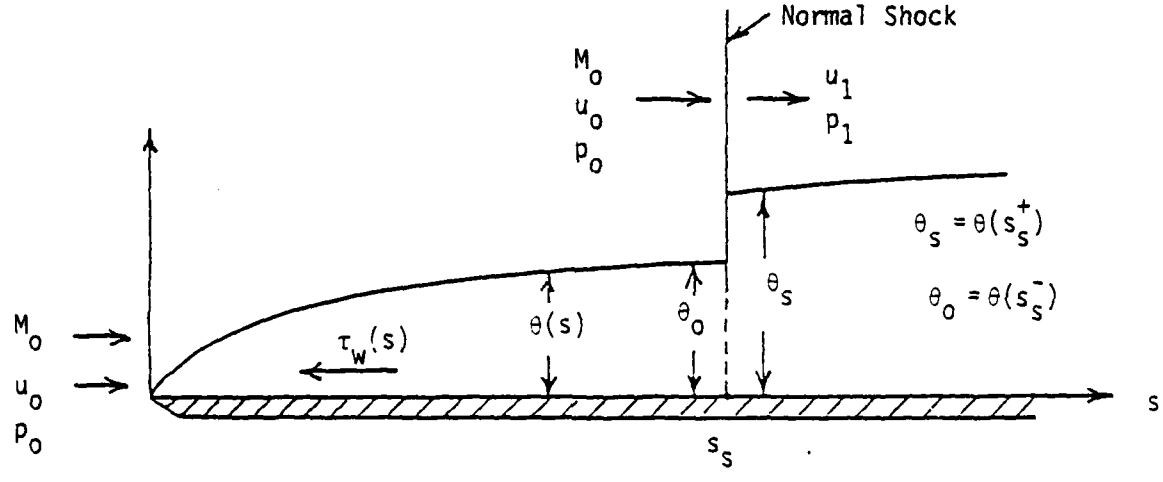

Figure C-2. A Simplified Flat Plate Boundary Layer Normal Shock Interaction Model

AD-A093 982 DYNAMICS TECHNOLOGY INC TORRANCE CA F/G 1/3
ANALYSIS FOR OBTAINING HIGH LIFT PRESSURE DISTRIBUTIONS FOR TRA--ETC(U)
JUN 80 E JAMES, K KUSUNOSE N00014-79-C-0458
UNCLASSIFIED DT-7817-6 NL

2 OF 2
AD A093982

END
DATE FILMED
2-81
DTIC

where $s^+ = \lim_{\varepsilon \to 0^+} (s_s + \varepsilon)$.

The pressure difference $(p_1 - p_0)$ appearing in equation (C-5) is approximated by the shock jump condition (C-3). This pressure difference is assumed invariant through the boundary layer to the leading order approximation. That is

$$\frac{(p_1 - p_0)}{\rho_0 u_0^2} = \frac{2}{(\gamma+1)} \left(1 - \frac{1}{M_0^2}\right) \; ; \; \begin{cases} s = s^+ \\ 0 \leq y \leq \delta(s^+) \end{cases} \tag{C-6}$$

The standard definition of the momentum thickness for flow over a flat plate is given by

$$\theta(s) \equiv \int_0^{\delta(s)} \frac{\rho u}{\rho_0 u_0} \left(1 - \frac{u}{u_0}\right) dy \tag{C-7}$$

From equations (C-4) and (C-7), the momentum thickness before the shock is given as an integral of the shear stress along the wall. That is,

$$\rho_o u_o^2 \theta_o \equiv \int_0^{s^-} \tau_w(\xi) d\xi \qquad \text{(C-8)}$$

where $s^- \equiv \underset{\varepsilon \to 0^-}{\text{Lim}} (s_s + \varepsilon)$

By combining equations (C-5) through (C-8), we can obtain an expression for the momentum thickness aft of the shock. If we denote it by θ_s, then

$$\theta_s = \frac{2}{(\gamma+1)} (1 - M_o^{-2}) \delta_s + \theta_o \qquad \text{(C-9)}$$

where $\delta_s \equiv \underset{\varepsilon \to 0^+}{\text{Limit}} \delta(s_s+\varepsilon)$ is the boundary-layer thickness aft of the shock. Equation (C-9) states that the jump in the momentum thickness across the shock is directly proportional to the boundary-layer thickness aft of the shock and to the pressure jump across the shock. The boundary-layer thickness δ_s can be written in terms of the boundary-layer thickness δ_o before the shock as

$$\delta_s = \delta_o (1+n) \qquad \text{(C-10)}$$

where n is generally a function of the Reynolds number $Re_s \left(\equiv \frac{u_o s_s}{\nu}\right)$ and the Mach number M_o. Inger and Mason [13] provide an expression for the jump in boundary-layer thickness across a shock. For Reynolds numbers in the range $10^6 \sim 10^7$, their development provides

$$n = 0.8 (M_o - 1) \qquad \text{(C-11)}$$

The boundary-layer thickness δ_o can, in turn, be related to the momentum thickness θ_o by assuming a power law expression for the velocity profile and substituting it into equation (C-7). That is, if

$$\frac{u}{u_o} = \left(\frac{y}{\delta_o}\right)^{1/\hat{k}} \qquad \text{(C-12)}$$

then equation (C-7) gives

$$\delta_o = \frac{(\hat{k}+1)(\hat{k}+2)}{\hat{k}\hat{g}} \theta_o \qquad \text{(C-13)}$$

where $\hat{g}$ is a compressibility factor (see Reference [8], Schlichting, pg. 674) ($\hat{g} \approx 0.713$ for $0.8 < M < 1.4$).

Substituting equations (C-10), (C-11) and (C-13) into (C-9) gives

$$\theta_s = \theta_o\left[1 + \frac{0.4(\hat{k}+1)(\hat{k}+2)}{(\gamma+1)\,\hat{k}\hat{g}} (1+4M_o)(1-M_o^{-2})\right] \qquad \text{(C-14)}$$

This is the principal result of this section. We have obtained an expression for the momentum thickness aft of a normal shock in terms of the known momentum thickness and flow conditions just before the shock. For typical values of $M_o \sim 1.2$, γ and $\hat{k}$, it can be shown that

$$\frac{\theta_s - \theta_o}{\theta_o} \sim O(1)$$

To apply this result to an arbitrary airfoil shape, we use the following expressions (obtained from equations (17) and (18) in the text of the report for the calculation of θ_o:

$$\theta_o = \begin{cases} \left[\dfrac{0.47\nu_o}{u_o}\displaystyle\int_0^{x_o}\left(\frac{u(\xi)}{u_o}\right)^5 d\xi\right]^{1/2} & \text{; full laminar run case} \\ (0.01475)^{4/5}\left(\dfrac{\nu_o}{u_o}\right)^{1/5}\left[\displaystyle\int_0^{x_o}\frac{u(\xi)}{u_o}^{3.94} d\xi\right]^{4/5} & \text{; turbulent case} \end{cases} \qquad \text{(C-15)}$$

where x_o is the arc-length location along the airfoil's upper surface where the peak velocity u_o occurs and which is also assumed to be the location of the shock wave. The reference condition [equations (C-15)] therefore correspond to conditions just before the shock.

Equivalent Flat Plate Length With a Normal Shock

With equation (C-14) it is now a simple matter to obtain the equivalent flat plate length with a shock. Consider the free stream conditions are u_1, ρ_1, ν_1, corresponding to conditions just aft of the normal shock wave. For steady flow past a flat plate, the wall shear stress and the momentum thickness are related by

$$\tau_w = \rho_1 u_1^2 \frac{d\theta}{ds} \tag{C-16}$$

When the free stream speed is near the sonic speed ($M_1 \sim 1$) and the boundary layer is turbulent, we can use the following empirical relationship [obtained by combining equations (C-16) and (19)] which relates the shear stress to the local Reynolds number, $Re_s = \frac{u_1 s}{\nu_1}$:

$$\tau_w = 0.036\ Re_s^{-1/6} \left(\frac{1}{2}\rho_1 u_1^2\right) \tag{C-17}$$

Equating equations (C-16) and (C-17) and solving for s as a function of θ gives the equivalent shock free flat plate length s_{so} as

$$s_{so} = \left(\frac{\theta_s}{(0.022)}\right)^{6/5} \left(\frac{u_1}{\nu_1}\right)^{1/5} \tag{C-18}$$

Since θ_s is proportional to θ_o and θ_o depends implicitly on the arc-length location x_o of the shock along the airfoil's upper surface (as given by equation (C-15)), then equation (C-18) provides the relationship between the equivalent flat plate length s_{so} and the shock location x_o on the airfoil. Figure C-3 illustrates graphically s_{so} and x_o.

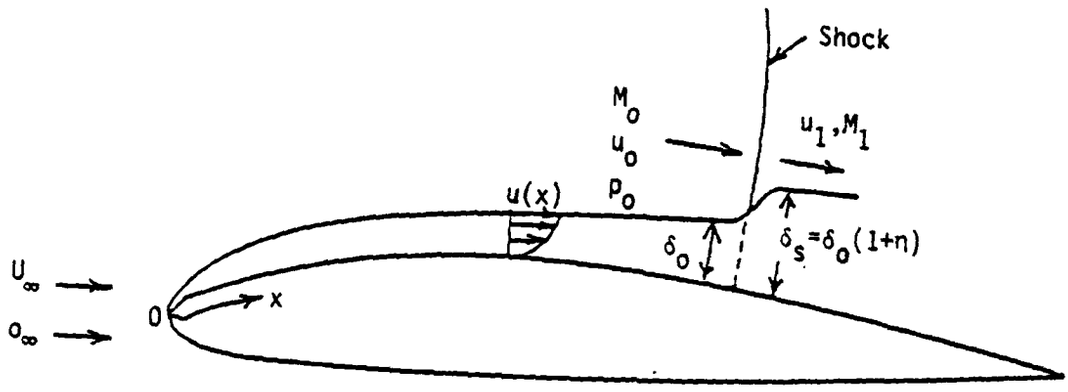

An Airfoil With a Shock in a Uniform Flow, u_∞, p_∞.

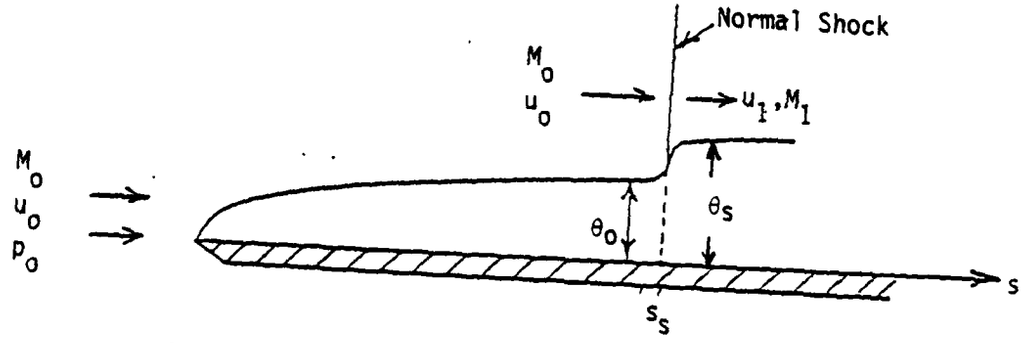

An Equivalent Turbulent Flat Plate With a Normal Shock.

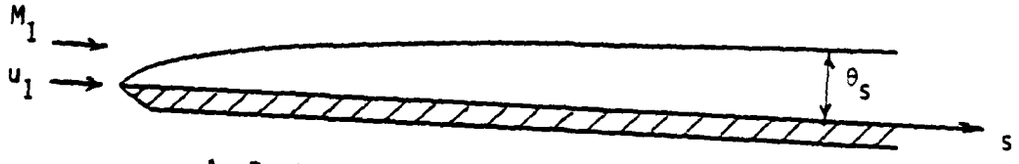

An Equivalent Turbulent Flat Plate

Figure C-3. An Arbitrary Airfoil and its Equivalent Turbulent Flat Plate

Incipient Separation With a Shock

The Stratford-type separation criterion developed previously can now be used to calculate a zero shear stress pressure recovery which includes the effect of a normal shock on the turbulent boundary layer. In order to obtain the pressure recovery which is on the verge of separation, a relationship is needed for the velocity profile before and after the shock.

Suppose the turbulent velocity profiles can be represented before and after the shock location as power law expressions. That is,

$$\frac{u}{u_o} = \left(\frac{y}{\delta_o}\right)^{1/\hat{k}} \qquad \text{(before shock)} \qquad \text{(C-19)}$$

$$\frac{u}{u_1} = \left(\frac{y}{\delta_s}\right)^{1/n} \qquad \text{(after shock)} \qquad \text{(C-20)}$$

where n and $\hat{k}$ are constants related by the shock strength from Gadd's analysis [7] as

$$n = (\hat{k}+3)\left(\frac{M_1}{M_o}\right)^2 - 3 \qquad \text{(C-21)}$$

Substituting the velocity profile (C-20) into the definition of the momentum thickness equation (C-7), gives [compare with equation (C-13)]:

$$\delta_s = \frac{(n+1)(n+2)}{n\hat{g}}\,\theta_s \quad ; \quad \hat{g} = 0.713 \qquad \text{(C-22)}$$

Consequently,

$$\frac{u}{u_1} = k_2\left(\frac{y}{\theta_s}\right)^m \qquad \text{(C-23)}$$

where $n \equiv 1/m$

$$k_2 \equiv \left[\frac{m\hat{g}}{(m+1)(2m+1)}\right]^m$$

The pressure recovery having zero surface stress can then be obtained from the separation criterion [equation (A-46)] by integrating the equation

$$[C_p^*]^{\frac{1}{4}(n-2)}\left(s\frac{dC_p^*}{ds}\right)^{1/2} = \tilde{g}(n)\ (R_{s1}10^{-6})^{1/12}\ ;\ s \geq s_{so},\ C_p^* \leq \frac{n-2}{n+1} \qquad (C\text{-}24)$$

where $R_{s1} = \dfrac{u_1 s}{\nu_1}$

$$C_p^* = \left(1 - \frac{u_e^2}{u_1^2}\right)$$

$$\tilde{g}(n) \equiv 21.32\left(\frac{3}{n^2(n+1)}\right)^{1/4}\left(\frac{n-2}{n+1}\right)^{\frac{n-2}{4}} \kappa k_1^{\,n/2} \Big/ \left(1 + r\frac{(\gamma-1)}{2}M_1^2\right)^{1/2}$$

$\kappa = 0.41$ Von Karman's constant

$k_1 = 0.683$ is an empirical constant obtained from turbulent flat plate experiments

$r = 0.9$ is the recovery factor for a turbulent boundary layer

Stratford Flows Starting with a Shock

To obtain the Stratford flows when a shock occurs at the location of the peak velocity, the same procedure used for the shockless case can be followed; namely to integrate equation (C-24) when $0 \leq C_p^* \leq \frac{n-2}{n+1}$ and use the momentum integral approach for $C_p^* \geq \frac{n-2}{n+1}$. In this procedure it becomes necessary to relate conditions at points downstream of the shock with conditions upstream of the shock. When this is the case, one assumes that along streamlines the isentropic assumption is valid everywhere except across the shock. The normal shock relations are used to relate conditions along the streamline across the shock location. Using the fact that the total enthalpy remains invariant all the way along a streamline (even across the shock), leads to the following C_p^* distribution [compare with equations (B-4) and (B-5)]:

$$C_p^* = B\left[\left(\frac{s}{s_{so}}\right)^{1/6} - 1\right]^{2/n} ; \quad 0 \leq C_p^* \leq \frac{n-2}{n+1} ,$$

where

$$\left.\begin{aligned} B &\equiv \left[\frac{3ng^2(n)\left(R_{s_{so}} \cdot 10^{-6}\right)^{1/6}}{1 + r\frac{\gamma-1}{2}M_1^2}\right]^{2/n} \\ R_{s_{so}} &\equiv \frac{u_1 s_{so}}{\nu_1} \end{aligned}\right\} \qquad \text{(C-25)}$$

and

$$C_p^* = 1 - (\alpha_3 s + \alpha_4)^{-1/2} ; \quad C_p^* \geq \frac{n-2}{n+1} \qquad \text{(C-26)}$$

where α_3, α_4 are determined by requiring C_p^* and $\frac{d}{ds} C_p^*$ from equations (C-25) - (C-26) match at $s = s_{sc}$. This matching gives [compare with equation (5)]:

$$\alpha_3 = \frac{2}{3}\left(\frac{n+1}{3}\right)^3 \frac{B}{n\, s_{sc}} \left[\left(\frac{s_{sc}}{s_{so}}\right)^{1/6} - 1\right]^{\frac{2-n}{n}} \left(\frac{s_{sc}}{s_{so}}\right)^{1/6}$$

$$\alpha_4 = \left(\frac{n+1}{3}\right)^2 - \alpha_3\, s_{sc} \qquad \text{(C-27)}$$

$$s_{sc} = s_{so}\left[1 + \left\{\frac{(n-2)}{B(n+1)}\right\}^{\frac{n}{2}}\right]^6$$

In these expressions n is selected on the basis of the Mach number jump across the shock according to:

$$n = (\hat{k}+3)\left(\frac{M_1}{M_o}\right)^3 - 3 \qquad \text{(C-28)}$$

where $2 \leq n \leq \hat{k}$ and $1/\hat{k}$ is the velocity power assumed for the shocked boundary layer profile just before the shock.

The speed ratio u_e/u_1 for *incipient separation* is obtained from equations (C-25) - (C-26) by

$$\frac{u_e}{u_1} = \sqrt{1 - C_p^*} \qquad \text{(C-29)}$$

REFERENCES

1. Stratford, B.D., *"The Prediction of Separation of the Turbulent Boundary Layer,"* Journal of Fluid Mechanics, Vol. 5, pp. 1-16, 1959.

2. Liebeck, R.H. and Smith, A.M.O., *"A Class of Airfoils Designed for High Lift Without Separation in Incompressible Flow,"* "Douglas Aircraft Report, MDC-J 1097/01, 1971.

3. Grabowski, W. *et al.*, *"Turbulent Flow Past a Self-Propelled Vehicle - Part I - Formulation,"* "Flow Research Report No. 69, December 1978.

4. Gadd, G.E., *"Interactions Between Normal Shock Waves and Turbulent Boundary Layers,"* Rand M. Report No. 3262, Ministry of Aviation - Aeronautical Research, Council of the Aerodynamic Division, N.P.L., 1962.

5. Smith, A.M.O., AGARD Report - Reference to be submitted next.

6. Walz, A., *"Anwendung des Energiesatzes von Wieghardt auf einparametrige Geschwindigkeitsprofile in Lamingren Grenzschichten,"* Ing.-Arc. Vol. 16, pp. 243-248, 1948.

7. Groschwitz, E., *"Caleul approche de la couche limite laminaire en ecoulement compressible sur une paroi nonconductrice de la ehaleur,"* (Office National d'Etudes et de Recherche Aeronautiques), Publication No. 40, Paris, 1950.

8. Schlichting, H. Boundary Layer Theory, Publ. McGraw-Hill, 1968.

9. Cebeci, T. and Smith, A.M.O., Analysis of Turbulent Boundary Layers, Publ. Academic Press, 1974.

10. NACA Report 1135

11. Clutter, D., *"Charts for Determining Skin Friction Coefficients on Smooth and on Rough Flat Plates at Mach Numbers up to 5 With and Without Heat Transfers,"* Douglas Aircraft Company, Inc., Report No. ES29074, 1959.

12. Liepman, H. and Roshko, A., Elements of Gas Dynamics, Publ. John Wiley & Sons, Inc., 1957.

13. Inger, G.R. and Mason, W.H., *"Analytical Theory of Transonic Normal Shock-Turbulent Boundary-Layer Interaction,"* AIAA, Vol. 14, No. 9.

DISTRIBUTION LIST FOR UNCLASSIFIED
TECHNICAL REPORTS AND REPRINTS ISSUED UNDER
CONTRACT N00014-79-C-0458 TASK 212-263

All addresses receive one copy unless otherwise specified.

Technical Library
Building 313
Ballistic Research Laboratories
Aberdeen Proving Ground, MD 21005

Mr. Aviars Celmins
Ballistic Research Laboratory
Ballistic Modelling Division
Aberdeen Proving Ground, MD 21005

Dr. P. J. Roache
Ecodynamics Research Associates, Inc.
P.O. Box 8172
Albuquerque, NM 87108

Defense Technical Information Center
Cameron Station, Building 5
Alexandria, VA 22314 12 copies

Library
Naval Academy
Annapolis, MD 21402

Director, Tactical Technology Office
Defense Advanced Research Projects Agency
1400 Wilson Boulevard
Arlington, VA 22209

Code 200B
Office of Naval Research
800 N. Quincy Street
Arlington, VA 22217

Code 438
Office of Naval Research
800 N. Quincy Street
Arlington, VA 22217 2 copies

Dr. J. L. Potter
Deputy Director, Technology
von Karman Gas Dynamics Facility
Arnold Air Force Station, TN 37389

Library
Aerojet-General Corporation
6352 North Irwindale Avenue
Azusa, CA 91702

NASA Scientific and Technical Information Facility
P.O. Box 8757
Baltimore/Washington International Airport, MD 21240

Dr. H. R. Chaplin
Code 1600
David W. Taylor Naval Ship Research and Development Center
Bethesda, MD 20084

Dr. Hans Lugt
Code 1802
David W. Taylor Naval Ship Research and Development Center
Bethesda, MD 20084

Dr. Francois Frenkiel
Code 1802
David W. Taylor Naval Ship Research and Development Center
Bethesda, MD 20084

Dr. T. C. Tai
Code 1606
David W. Taylor Naval Ship Research and Development Center
Bethesda, MD 20084

Dr. George R. Inger, Chairman
Department of Aerospace Engineering
University of Colorado
Boulder, Colorado 80309

Professor C. H. Lewis
Department of Aerospace and Ocean Engineering
Virginia Polytechnic Institute and State University
Blacksburg, VA 24061

Dr. A. Rubel
Research Department
Grumman Aerospace Corporation
Bethpage, NY 11714

Commanding Officer
Office of Naval Research Eastern/Central
Regional Office
666 Summer Street, Bldg. 114, Section D
Boston, MA 02210

Dr. J. C. Erickson, Jr.
CALSPAN Corporation
Advanced Technology Center
P.O. Box 400
Buffalo, NY 14225

Dr. C. Witliff
CALSPAN Corporation
Advanced Technology Center
P.O. Box 400
Buffalo, NY 14225

Commanding Officer
Office of Naval Research Branch Office
536 South Clark Street
Chicago, IL 60605

Code 753
Naval Weapons Center
China Lake, CA 93555

Mr. J. Marshall
Code 4063
Naval Weapons Center
China Lake, CA 93555

Library MS 60-3
NASA Lewis Research Center
21000 Brookpark Road
Cleveland, OH 44135

Dr. J. D. Anderson, Jr.
Chairman, Department of Aerospace
Engineering
College of Engineering
University of Maryland
College Park, MD 20742

Professor O. Burggraf
Department of Aeronautical and
Astronautical Engineering
Ohio State University
1314 Kinnear Road
Columbus, OH 43212

Technical Library
Naval Surface Weapons Center
Dahlgren Laboratory
Dahlgren, VA 22448

Dr. F. Moore
Naval Surface Weapons Center
Dahlgren Laboratory
Dahlgren, VA 22448

Technical Library 2-51131
LTV Aerospace Corporation
P.O. Box 5907
Dallas, TX 75222

Library, United Aircraft Corporation
Research Laboratories
Silver Lane
East Hartford, CT 06108

Library (MS 185)
NASA Langley Research Center
Langley Station
Hampton, VA 23665

Professor A. Chapmann
Chairman, Mechanical Engineering Department
William M. Rice Institute
Box 1892
Houston, TX 77001

Technical Library
Naval Ordnance Station
Indian Head, MD 20640

Professor D. A. Caughey
Sibley School of Mechanical and
Aerospace Engineering
Cornell University
Ithaca, NY 14850

Professor E. L. Resler
Sibley School of Mechanical and
Aerospace Engineering
Cornell University
Ithaca, NY 14850

Professor S. F. Shen
Sibley School of Mechanical and
Aerospace Engineering
Cornell University
Ithaca, NY 14850

Library
Midwest Research Institute
425 Volker Boulevard
Kansas City, MO 64110

Dr. J. J. Riley
Flow Research, Inc.
P.O. Box 5040
Kent, WA 98031

Dr. S. A. Orszag
Cambridge Hydrodynamics, Inc.
54 Baskin Road
Lexington, MA 02173

Professor J. D. Cole
Mechanics and Structures Department
School of Engineering and Applied Science
University of California
Los Angeles, CA 90024

Engineering Library
University of Southern California
Box 77929
Los Angeles, CA 90007

Commanding Officer
Naval Ordnance Station
Louisville, KY 40214

Mr. B. H. Little, Jr.
Lockheed-Georgia Company
Department 72-74, Zone 369
Marietta, GA 30061

Professor E. R. G. Eckert
University of Minnesota
241 Mechanical Engineering Building
Minneapolis, MN 55455

Dr. Gary Chapman
Mail Stop 227-4
Ames Research Center
Moffett Field, CA 94035

Library
Naval Postgraduate School
Monterey, CA 93940

Dr. S. S. Stahara
Nielsen Engineering and Research, Inc.
510 Clyde Avenue
Mountain View, CA 94043

Engineering Societies Library
345 East 47th Street
New York, NY 10017

Professor A. Jameson
Courant Institute of Mathematical Sciences
New York University
251 Mercer Street
New York, NY 10012

Professor G. Miller
Department of Applied Science
New York University
26-36 Stuyvesant Street
New York, NY 10003

Office of Naval Research
New York Area Office
715 Broadway - 5th Floor
New York, NY 10003

Mr. D. Farmer
Naval Ocean Research and Development Activity
Code 332
NSTL Station, MS 39522

Librarian, Aeronautical Library
National Research Council
Montreal Road
Ottawa 7, Canada

Lockheed Missiles and Space Company
Technical Information Center
3251 Hanover Street
Palo Alto, CA 94304

Commanding Officer
Office of Naval Research,
Western Regional Office
1030 East Green Street
Pasadena, CA 91106

Engineering Division
California Institute of Technology
Pasadena, CA 91109

Library
Jet Propulsion Laboratory
4800 Oak Grove Drive
Pasadena, CA 91103

Mr. L. I. Chasen, MGR-MSD Library
General Electric Company
Missile and Space Division
P.O. Box 8555
Philadelphia, PA 19101

Technical Library
Naval Missile Center
Point Mugu, CA 93042

Professor S. Bogdonoff
Gas Dynamics Laboratory
Department of Aerospace and
Mechanical Sciences
Princeton University
Princeton, NH 08540

Professor S. I. Cheng
Department of Aerospace and
Mechanical Sciences
Princeton University
Princeton, NH 08540

Dr. J. E. Yates
Aeronautical Research Associates
of Princeton, Inc.
50 Washington Road
Princeton, NH 08540

Professor L. Sirovich
Division of Applied Mathematics
Brown University
Providence, RI 02912

Redstone Scientific Information Center
Chief, Document Section
Army Missile Command
Redstone Arsenal, AL 35809

U. S. Army Research Office
P.O. Box 12211
Research Triangle, NC 27709

Editor, Applied Mechanics Review
Southwest Research Institute
8500 Culebra Road
San Antonio, TX 78228

Library and Information Services
General Dynamics - CONVAIR
P.O. Box 1128
San Diego, CA 92112

Dr. R. Magnus
General Dynamics - CONVAIR
Kearny Mesa Plant
P.O. Box 80847
San Diego, CA 92138

Office of Naval Research
San Francisco Area Office
One Hallidie Plaza, Suite 601
San Francisco, CA 94102

Library
The RAND Corporation
1700 Main Street
Santa Monica, CA 90401

Dr. P. E. Rubbert
Boeing Aerospace Company
Boeing Military Airplane Development
Organization
P.O. Box 3707
Seattle, WA 98124

Dr. H. Yoshihara
Boeing Aerospace Company
P.O. Box 3999
Mail Stop 41-18
Seattle, WA 98124

Librarian
Naval Surface Weapons Center
White Oak Laboratory
Silver Spring, MD 20910

Engineering Library
McDonnell Douglas Corporation
Department 218, Building 101
P.O. Box 516
St. Louis, MO 63166

Dr. R. J. Hakkinen
McDonnell Douglas Corporation
Department 222
P.O. Box 516
St. Louis, MO 63166

Dr. N. Malmuth
Rockwell International Science Center
1049 Camino Dos Rios
P.O. Box 1085
Thousand Oaks, CA 91360

Library
Institute of Aerospace Studies
University of Toronto
Toronto 5, Canada

Professor A. R. Seebass
Department of Aerospace and
Mechanical Engineering
University of Arizona
Tucson, AZ 85721

Dr. K. T. Yen
Code 3015
Naval Air Development Center
Warminster, PA 18974

Air Force Office of Scientific
Research (SREM)
Building 1410, Bolling AFB
Washington, DC 20332

Chief of Research and Development
Office of Chief of Staff
Department of the Army
Washington, DC 20310

Library of Congress
Science and Technology Division
Washington, DC 20540

Director of Research (Code RR)
National Aeronautics and Space
Administration
600 Independence Avenue, SW
Washington, DC 20546

Library
National Bureau of Standards
Washington, DC 20234

National Science Foundation
Engineering Division
1800 G Street, NW
Washington, DC 20550

AIR 320D
Naval Air Systems Command
Washington, DC 20361

AIR 950D
Naval Air Systems Command
Washington, DC 20375

Code 2627
Naval Research Laboratory
Washington, DC 20375

SEA 03512
Naval Sea Systems Command
Washington, DC 20362

SEA 09G3
Naval Sea Systems Command
Washington, DC 20362

Dr. Charles Watkins
Head, Mechanical Engineering Department
Howard University
Washington, DC 20059

Dr. A. L. Slafkosky
Scientific Advisor
Commandant of the Marine Corps
Code AX
Washington, DC 20380

Director
Weapons Systems Evaluation Group
Washington, DC 20350

Research Library
AVCO Corporation
Missile Systems Division
201 Lowell Street
Wilmington, MA 01887

AFAPL (APRC)
AB
Wright Patterson AFB, OH 45433

Dr. Donald J. Harney
AFFDL/FX
Wright Patterson AFB, OH 45433